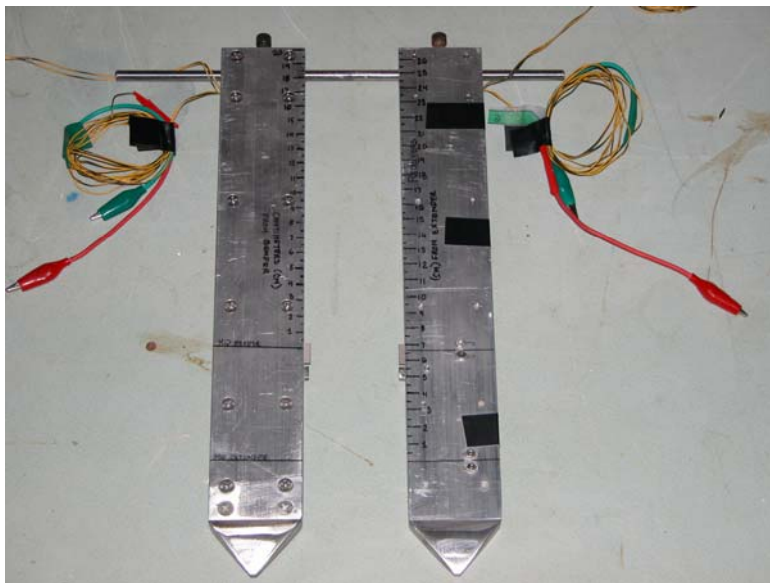# Cone Penetrometer Equipped with Piezoelectric Sensors for Measurement of Soil Stiffness in Highway Pavement

Xiangwu (David) Zeng and Heather Hlasko
Department of Civil Engineering, Case Western Reserve University

1. Report No. FHWA/OH-2005/15	2. Government Accession No.	3. Recipient's Catalog No.
4. Title and subtitle Cone Penetrometer Equipped with Piezoelectric Sensors for Measurement of Soil Stiffness in Highway Pavement		5. Report Date November 2005
		6. Performing Organization Code
7. Author(s) Xiangwu (David) Zeng		8. Performing Organization Report No.
9. Performing Organization Name and Address Case Western Reserve University Case School of Engineering Department of Civil Enigneering 10900 Euclid Avenue Cleveland, OH 44106		10. Work Unit No. (TRAIS)
		11. Contract or Grant No. 134185
		13. Type of Report and Period Covered
12. Sponsoring Agency Name and Address Ohio Department of Transportation 1980 West Broad Street Columbus, Ohio 43223		14. Sponsoring Agency Code
15. Supplementary Notes		

16. Abstract

The stiffness (elastic modulus and shear modulus) and Poisson's ratio of the base and sublayers are important parameters in the design and quality assurance during construction of highway pavements. The new highway construction guide proposed by AASHTO (American Association for State Highway and Transportation Officials) recommends such measurements be conducted.

A new field-testing technique has been developed in the geotechnical laboratory of Case Western Reserve University to measure the stiffness and Poisson's ratio of soils using cone penetrometers equipped with piezoelectric sensors. We developed the technique into a low cost, automated and mobile unit that can be widely used during highway construction for monitoring and controlling construction quality of highway pavements and for evaluating performance of existing pavements. The system is mobile, versatile, user friendly, and applicable to all types of soils and field conditions. Preliminary tests in the laboratory show that the design objectives of this device have been achieved.

17. Key Words Cone Penetrometers, Piezoelectric Sensors, Soil Stiffness, Highway Pavement		18. Distribution Statement No restrictions. This document is available to the public through the National Technical Information Service, Springfield, Virginia 22161	
19. Security Classif. (of this report) Unclassified	20. Security Classif. (of this page) Unclassified	21. No. of Pages	22. Price
Form DOT F 1700.7 (8-72)	Reproduction of completed pages authorized		

CHAPTER ONE
INTRODUCTION

1.0   Objectives of This Project

The objectives of the proposed study are:

1) To improve the mechanical system of the device to make it applicable to complex and challenging field conditions. It will be mobile, robust, water proof, and applicable to all types of conditions possible in the field.

2)   To improve the data acquisition system and the software for automated data analysis. We developed a user-friendly program to calculate the elastic modulus, shear modulus, and Poisson's ratio based on the reading from the wave tests and the results will be shown on the screen in a few minutes.

3)   To conduct laboratory tests on a wide range of soils to check the system and to validate the results.

1.1   History of Pavement Development

The history of road construction began more than 1800 years ago when the Romans established the trade. Although they were nowhere near the quality of the highways that are being constructed today, the Romans laid out nearly 4,828 kilometers (3,000 miles) of principal roadways within only a 150 year time-frame. Even with the technology and construction equipment used to build highways today, this amount in such a short time span is quite impressive. These Roman roadways spanned across the country, extending into the heart of Wales and north as far as Hadrian's Wall [9]. The Romans constructed their roads so efficiently that portions of them remain in tact and functional today.

The roads in Europe began solely as Roman military entities and had no economic function in the lives of the native people. In every region, including Italy, that the Romans conquered, they built roadways. The structure of the roads did not vary excluding the thicknesses, which were modified to account for the strength of the foundation. Two trenches were dug approximately five meters (16.4 feet) apart to serve as drainage ditches, and the soil between was excavated down to a competent foundation on which a multilayer granular base was laid using materials locally available [9]. Roman roads were generally straight, even over steep grades. The pavements were sometimes modified aesthetically by adding a surface of flat quarried stone, which rested on a bed of smaller stones.

As agriculture improved and market towns began to develop, the need for roads quickly accelerated. With the need for roads came the desire to improve the quality of travel and with this desire came advancement in pavement technology. Throughout the early portion of the 19th century, compaction of granular pavements was left to the traffic. This method created ruts and uneven surfaces which usually ended up retaining water and creating small ponds. In the 1830's France first began implementing rolling as a part of the construction process. These rollers were typically horse-drawn and difficult to control. The 1860's saw the development of steam rollers such as the one depicted below (Figure 1.1) which significantly increased the quality of compaction.

As compaction techniques improved so too did the surfacing for roads. Throughout Europe during the medieval times, stone setts were the most popular form of pavement construction in towns and cities. However, this construction method did not gain the popularity in the United States that it held in Europe. American roads were constructed of hard-burnt bricks, preferred for their regularity and homogeneity.

Asphalt pavements were first constructed in Paris in 1858, when the Rue Begere was surfaced with Val de Travers asphalt [9]. This asphalt was produced by crushing natural limestone infused with bitumen. It soon became the preferred method of paving and by 1875 most of the major commercial roads of the city had surfacings of this Val de Travers asphalt. However, asphalt surfacings did not fashion themselves in the United Stated until well after the 1870's.
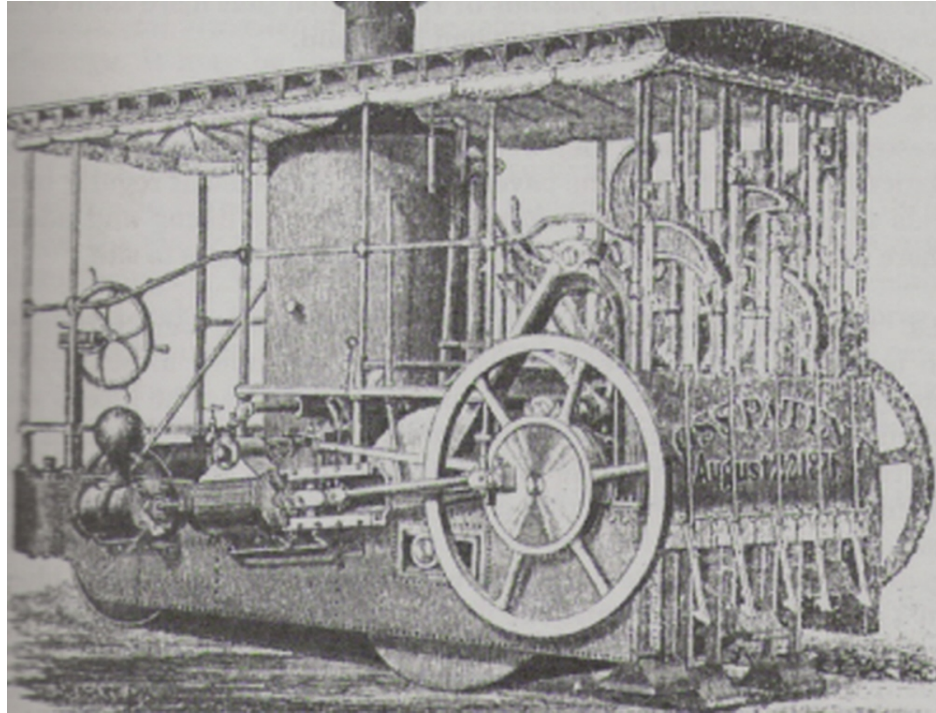
Figure 1.1   The Ross Ramming Machine [9].

Eventually, as the popularity of asphalt surfacings in the United States increased throughout the 19th century, it became common knowledge that the surfacing itself made no noteworthy contribution to the actual strength of the pavement. Although pavements since developed are greatly advanced in composition and quality, this theory still holds true today. It is indeed the function of the underlying foundation to provide the strength for the pavement itself.

In the United States today, the Interstate Highway System consists of 68,869 kilometers (42,793 miles) of roads connecting every major city. Other familiar road networks which serve to unify large areas include Germany's Autobahn, the Trans-Canada Highway, and the Pan-American Highway. In 2004, a 23-nation agreement to link Asia with a network of highways was signed.

Currently, the cause of premature failure in many pavements is that of poor construction. The quality of compaction is the greatest factor in determining pavement performance. Inadequate compaction results in a pavement with decreased stiffness, reduced fatigue life, accelerated aging, decreased durability, rutting, raveling, and moisture damage [8]. As a result, the significance of quality control and quality assurance is being implemented more than ever before.

Along with quality control and quality assurance, the measurement of in-situ soil properties is imperative for a lasting pavement design. The stiffness (elastic modulus and shear modulus) and Poisson's ratio of the base and sublayers are essential factors in the design and quality control / quality assurance of compaction during the construction of highway pavements. Both during and after the construction of a highway pavement, it is critical and lucrative to have a portable and mechanized system that can measure these parameters of in-situ compacted soils efficiently. The new highway construction guide proposed by the American Association for State Highway and Transportation Officials (AASHTO) in 2004 presents the necessity that such measurements be carried out. In addition, the final report for NCHRP 1-37A (the National Cooperative Highway Research Program) deems such measurements "crucial" [32]. Today's currently used techniques such as CBR (California Bearing Ratio), resilient modulus, DCP (Dynamic Cone Penetrometer), and FWD (Falling Weight Deflectometer) tests have individual confines that prevent them from complying with all of the requirements for the design and quality control / quality assurance of highway pavements.

1.2   Currently Used Techniques

In the structural design of a highway pavement, the stiffness (elastic modulus and shear modulus) of the subgrade and its Poisson's ratio are of utmost importance. However, these properties are not easy to measure. Engineers must always consider the inconsistency and the variability of soils over relatively small distances. Therefore, it is currently not cost effective to use those properties directly to consider subgrade suitability. Today's pavements are generally designed empirically on past experience or fundamentally using elastic theory. This allows relatively simple test procedures to be implemented, the results of which can be related by experiment to the structural properties of the subgrade. The following sections describe the current soil stiffness testing methods.

1.2.1   California Bearing Ratio (CBR)

One currently used test procedure and probably the most popular as well is known as the California Bearing Ratio (CBR). The CBR test was first developed in the 1920's and was modified by the U.S. Army Corps of Engineers for airfield design in the early 1940's. This test method is used specifically to evaluate the potential strength of the subgrade, subbase, and base course material for use in road pavements. However, as with many tests developed and modified over an extensive period of time, the methods of sample preparation and testing itself has fluctuated considerably over the years. Currently the equipment and test procedure are described in detail in BS 1377:1975, Test 16, and under AASHTO

Designation T193-81 (1986) [9]. The following figure (Figure 1.2) depicts the equipment used in the CBR testing procedure.

The basic test consists of causing a plunger of standard cross-sectional area to penetrate a designated soil sample. The soil to be tested is compacted into the mould at the moisture content and dry density which it is assumed will be attained in the prepared subgrade. The penetration test is then carried out at a standard rate. A loading frame is used to give the required reaction and a proving ring measures the load. This load required to cause the penetration is plotted against the measured penetration itself. This plot establishes the CBR value of the soil tested.
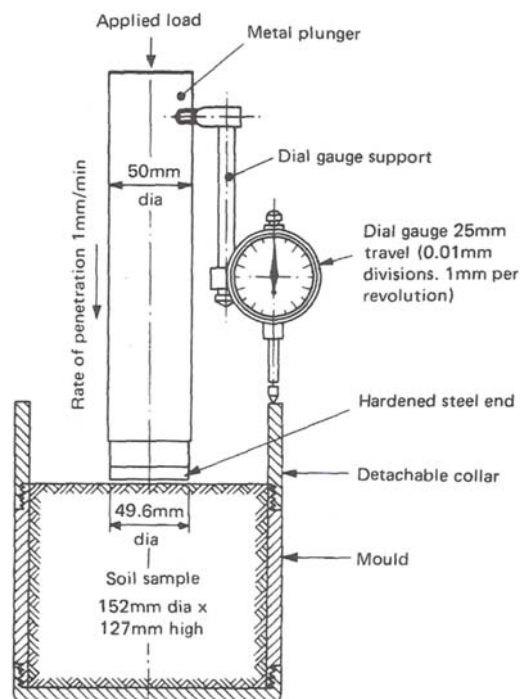

Figure 1.2   California Bearing Ratio (CBR) test equipment.

Typical load-penetration curves are shown in Figure 1.3. The loads required to cause penetrations of 2.5 and 5 millimeters (.098 and .197 inches, respectively) are recorded and expressed as ratios of the loads to cause the same penetrations in a well-graded crushed stone, the load-penetration curve for which is also included in Figure 1.3. It is a basic comparison between the bearing capacity of a subgrade material with that of a standard crushed rock material. This standard arises from the fact that the test was originally designed to asses the quality of fine crushed-rock base materials in the state of California. Thus, a high quality crushed stone material should have a CBR of 100 percent. The following table provides a general relationship between CBR values and the general subgrade strength.

Table 1.1 CBR Value Vs. Subgrade Strength [7].

CBR Value	Subgrade Strength
3% and less	Poor
3% - 5%	Normal
5% - 15%	Good

As can be seen for "Test 2" in the following diagram (Figure 1.3), the first part of the penetration curve may exhibit concave properties. When this occurs,

> "The load-penetration curve is projected back to the horizontal axis to give the intercept "A", as shown in the figure. This intercept is added to the standard penetrations of 2.5 and 5 mm when evaluating the loads equivalent to those penetrations for the materials under test. However, no addition is made in obtaining the corresponding loads for the standard crushed stone material. The larger of the ratios corresponding to the 2.5 and 5 mm penetrations is normally taken as the CBR value of the material for the test conditions used [9]."

The CBR test method is generally intended for evaluating the strength of cohesive materials having maximum particle sizes less than 19 mm or ¾-in [25]. The test is recommended for, but is not limited to this size specification. Generally speaking, if the sample to be tested contains 10 percent or less (by weight) coarser than 19 mm (¾-in) then this portion can be removed without drastically miscalculating the actual strength of the soil. However, this test is not applicable for soils containing greater than 10 percent (by weight) coarser than 19 mm (¾-in). When this occurs, tests on the fraction passing 19 mm (¾-in) can be carried out at a range of various moisture contents. This will give a broad indication of whether the material as a whole will lose strength if the moisture content is increased.

Generally, the CBR test is carried out in a laboratory environment, but it can also be carried out in situ. Rigs designed to fit at the rear of suitably loaded site vehicles are currently available. However, there is a clear difference in the degree of confinement of the soil in laboratory tests versus those conducted in situ. This difference in the confinement has a large effect on the stress distribution under the plunger, and therefore on the resulting load-penetration curves. It has been generalized that for heavy clays and for other cohesive soils having an air content of 5 percent or more, the difference between the results of laboratory tests and those of tests in situ is trivial. On the other-hand, for other cohesive soils and the majority of granular materials the difference is much greater. In this case, the results of the tests in situ should not be used to verify the quality control / quality assurance in relation to specification requirements.
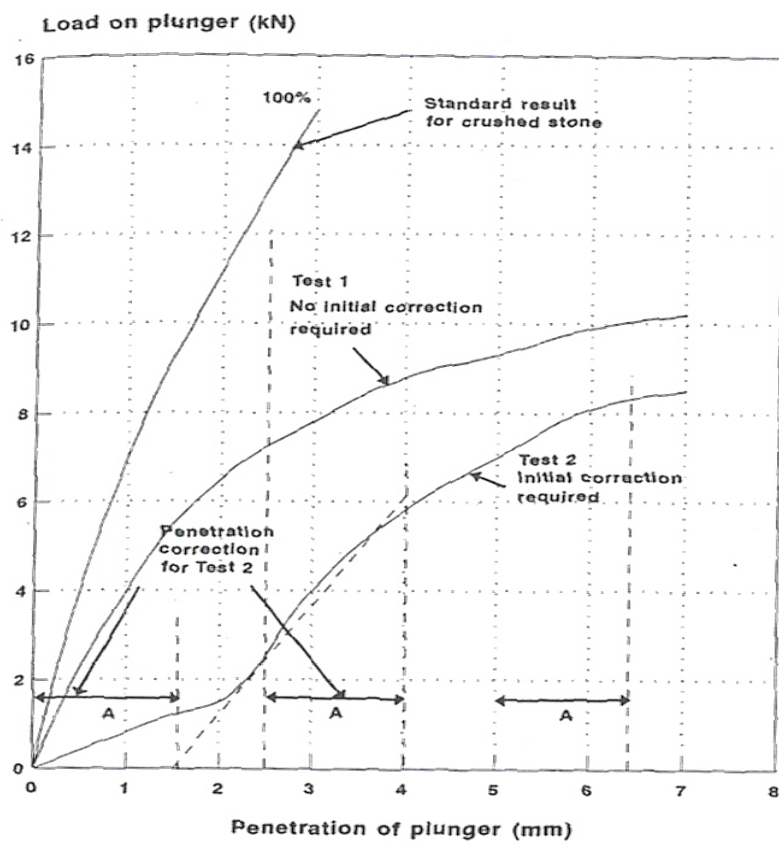

Figure 1.3   Typical CBR test results.

1.2.2   Resilient Modulus

In the past, pavement designers and engineers have been dependent upon static testing techniques such as the California Bearing Ratio method of the previous section. However, with increased technology and improved testing techniques, increased emphasis has been placed on repeated load testing to better replicate the characteristics of traffic loading. Therefore, the resilient modulus test (AASHTO T-247-

82) has become the center of attention in the world of pavement design. Resilient modulus (M_R) is basically a measure of stiffness. Currently, the resilient modulus of soils or other materials can be determined, estimated or back-calculated in the laboratory or in the field.

This test applies a repeated axial cyclic stress of fixed magnitude, load duration, and cycle duration to a cylindrical test specimen. While the test specimen is being subjected to this dynamic cyclic stress, it is also being subjected to a static confining stress provided by a triaxial pressure chamber. This test is essentially a cyclic version of a triaxial compression test where the cyclic load application is considered to more accurately simulate authentic traffic loading conditions. More specifically, in the laboratory,

> "A triaxial test is taken up to some stress level, say, 0.25 to 0.50 of the estimated ultimate value; then the deviator load is reduced to zero and then reapplied. This load cycling is repeated three to five times; on the last cycle the deviator load is then continued to sample failure (see Figure 1.4). There is some body of opinion that the initial tangent modulus (which is somewhat larger than on the initial cycles, with the increase considered due to strain hardening) is a better estimate of the stress-strain modulus (or modulus of elasticity) than otherwise obtained. This initial tangent modulus is termed the resilient modulus to distinguish it from one obtained from the usual triaxial compression test [5]."
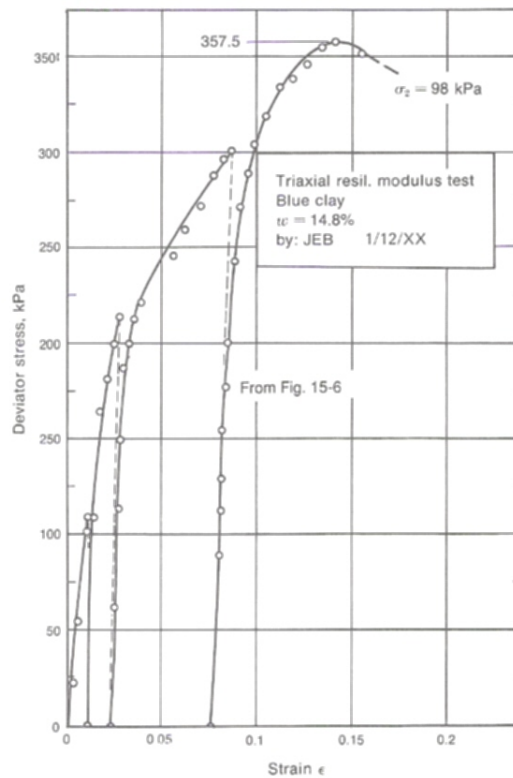
Figure 1.4   Resilient modulus test from edited stress-strain data.

In addition, there are many correlation equations between the California Bearing Ratio (CBR) and the resilient modulus (M_R). However, each one has its limitations, which should be noted and taken into consideration during pavement design. Table 1.2 present some of the more popular correlation equations and their limitations.

Table 1.2   Selected subgrade strength/stiffness correlation equations

Equation	Origin	Limitations
$M_R = 1,500*(CBR)$	Heukelom & Klomp (1962)	Only for fine-grained non-expansive soils with a soaked CBR or 10 or less.
$M_R = 2,555*(CBR)^{0.64}$	AASHTO 2002 Design Guide	A fair conversion over a wide range of values.

1.2.3   Dynamic Cone Penetrometer (DCP)

The Dynamic Cone Penetrometer (DCP), originally created in 1959 by the late Professor George F. Sowers, is an instrument which can be used for the immediate measurement of the in situ strength of fine grained and granular subgrades, granular base and subbase materials, and weakly cemented materials.

A schematic of the Dynamic Cone Penetrometer is shown in Figure 1.5(b). The DCP is essentially a long steel rod with a standard size hardened steel cone at the penetrating end. It is approximately two meters in length, but it can be lengthened by adding extension rods. At the upper end of the steel bar, surrounding the rod is a captive weight. This weight is able to freely fall through a prescribed drop height to achieve a standard amount of penetrative energy at each drop.

A "resistance vs. penetration" plot is created by measuring the penetration of the cone against the number of drops of the weight. Indirectly the strength/compaction of the layer being tested is determined. The idea is similar to that of a Standard Penetration Tests (SPT), which provides a measure of resistance of the soil to penetration, in terms of the number of blows (N). Figure 1.6 shows the general schematic of a SPT test in progress.
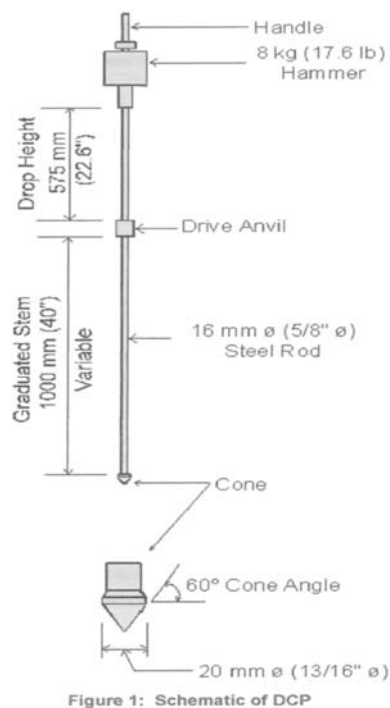

Figure 1: Schematic of DCP

Figure 1.5   **(a)** Typical DCP used in the field. **(b)** Schematic of DCP.
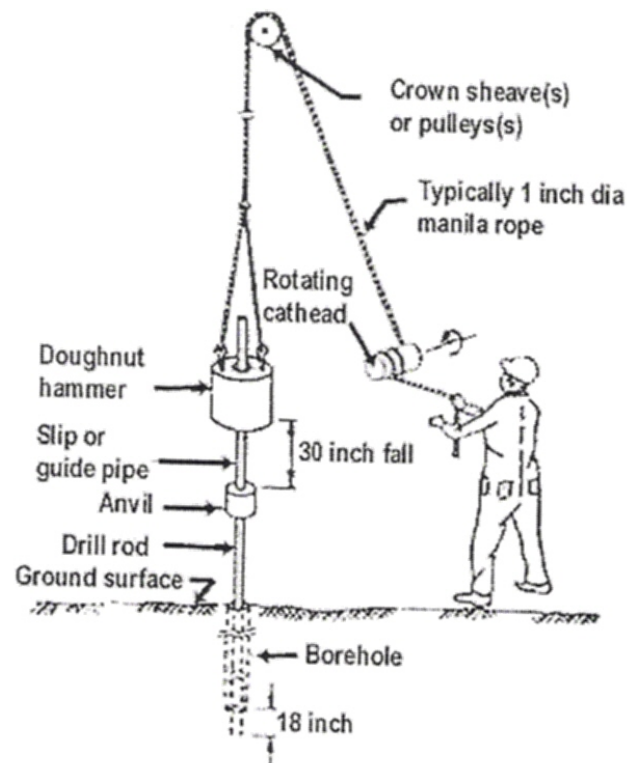
Figure 1.6   SPT test in progress.

DCP testing can be performed on site.   The steel rod can directly penetrate through thin flexible pavements with uncemented aggregate sublayers, such as many "oil and chip" pavements or can be used to test through lightly cemented materials having unconfined compressive strengths of less than 3,000 kPa (440 psi).   For any other materials exceeding this strength, DCP testing can only be completed after a core containing this material is removed.

1.2.4   Falling Weight Deflectometer (FWD)

The falling weight deflectometer, or FWD, is a non-destructive testing device used to evaluate the physical properties of a given section of pavement.   The FWD machine is usually contained within a trailer that is driven to a location by means of another vehicle.   At a pre-designated change in distance, the FWD device is deployed (see Figures 1.7 and 1.8(a)).

Figure 1.7 FWD device.

In the United States today, the most commonly used FWD is known as the Dynatest Model 8000 FWD system [17]. This FWD is a pavement loading device capable of delivering a transient force impulse representative in magnitude and duration to moving truck wheel loads. The Dynatest Model 8000 delivers this load impulse to the pavement surface by dropping a weight of 50, 100, 200, or 300 kilograms (110, 220, 440, or 660 pounds, respectively) from a height of approximately 2 to 38 cm (0.8 to 15 inches) (see Figure 1.8(b)). A peak force ranging from 680 to 10,900 kilograms (1,500 to 24,000 pounds) can be generated by varying the mass or the drop height or both. The load is conveyed to the pavement through a loading plate which provides a load pulse in the form of a half sine wave. The magnitude of load is measured by the load cell [17].

Vertical deformations are measured by seven mounted deflection sensors which can be automatically lowered to the pavement surface along with the loading plate. One of the sensors or velocity transducers is located at the center of the loading plate, while the remaining six can be positioned up to 2.3 meters (7.4 feet) from the center. The Dynatest FWD is also equipped with a microprocessor-based control console that can conveniently fit on the passenger side of the front seat [17].
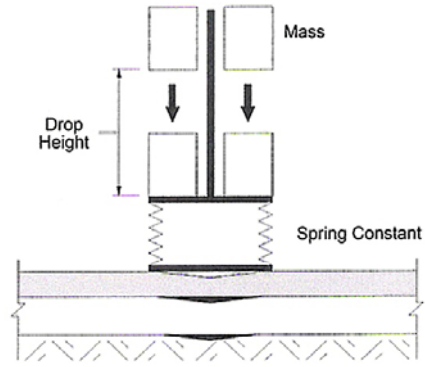
Figure 1.8 **(a)** FWD trailer. **(b)** FWD load applied to pavement.

Other infrequently used commercial falling weight deflectometer tests include the KUAB FWD and the Pheonix FWD.

1.3 Limitations to the Current Testing Methods

The American Association for State Highway and Transportation Official's *Guide for the Design of Pavement Structures* is the principle text that is used in the design of new and rehabilitated highway pavements. This guide was centered around the experimental design approaches drawn from the AASHO Road Test. These design approaches are very limited in that they only deal with structural sections at a single location and with narrow traffic levels compared to larger traffic levels of the present day. Currently, emphasis is shifting from design and construction of highways to rehabilitation of older highways. The majority of the empirical design approaches and testing methods, including those previously described, are generally insufficient for this new area of focus. To compensate for the lack of sufficiency, mechanistic design approaches have been combined with the current empirical approaches. Mechanistic-empirical approaches more sensibly characterize working pavements and enhance the dependability of designs. In the near future, design approaches will be based solely on mechanistic principles. However, because of the current breach that is present in today's knowledge base, mechanistic design methods must be supported by empirical relationships. It had been concluded by AASHTO that the mechanistic-empirical design approach needs to be much better defined before practical and realistic design procedures can be developed and implemented [22]. Hence the development of a "Guide for the Design of New and Rehabilitated Pavement Structures", based on M-E principles, and accompanied by the necessary software, for adoption and distribution by AASHTO has begun.

More specifically, the problems and shortcomings associated with the testing methods previously mentioned in Section 1.2 are as follows: First, the majority of the testing methods use samples of the base, subbase, and subgrade layers that have been prepared and compacted in the laboratory using procedures that are very different from what the soils are subjected to in-situ. The laboratory compacted specimens may possibly have stiffnesses different from the soils compacted in the field. The quality of laboratory tests in their ability to provide accurate measurements of soil properties depends greatly on the ability to recreate the conditions found in the field. Secondly, most of these tests require soil sampling which in some cases may be too difficult to obtain due to the location of the subject project site with respect to both structural safety and personal safety. On the other hand, if it is possible to obtain a sample, it is highly likely that the sample be severely disturbed through the sampling process itself, which ultimately provides inaccurate testing results. Third, these tests do not offer the specific pieces of information needed by engineers and pavement designers to establish whether the stiffness of pavement materials and soils under construction (in the field) meet the design constraints. In addition, for an existing pavement where the subgrade, subbase, and the base soils have experienced years of weathering and traffic loading applications, the current testing methods are not capable of determining the stiffness of these in-situ soils. Finally, the value of Poisson's ratio is an extremely valuable consideration in pavement design calculations. Currently, the value of Poisson's ratio is being estimated rather than measured in most design cases [32]. This presents a great need to develop a non-destructive, accurate and economical field test for the measurement of stiffness (elastic and shear modulus) and Poisson's ratio for the underlying soils of pavements. The new highway construction guide mentioned earlier in this paragraph, which was proposed by AASHTO and supported by the final report for the National Cooperative Highway Research Program (NCHRP) 1-37A requires such "key" testing methods.

1.4   Implementation of a New Testing Device

At the present time, there is no such testing device on the market which can dependably measure the stiffness of in-situ base and subgrade layers during and after pavement construction. However, a new field-testing technique has recently been developed by Dr. Xiangwu Zeng of Case Western Reserve University to measure small-strain moduli (elastic and shear modulus) and Poisson's ratio of soils [32]. This new technique employs the bender and extender element method. The device includes a pair of cone penetrometers, which are each fitted with two piezoelectric sensors for a total of four sensors (or two pairs of sensors). This device can be pressed into foundation soils through the simple application of a vibratory hammer. One set of the piezoelectric sensors (one penetrometer) is used as wave

transmitters while the other set (the other penetrometer) is used as wave receivers. An electrical pulse produced by a function generator is used to stimulate the transmitters. Vibration of the transmitters produces primary and shear waves (p- and s-waves) that disseminate through the soil sample and are seized by the receivers. From the measured velocities of the s- and p-waves, soil stiffness and Poisson's ratio can be determined. Thus far, this cone penetrometer - piezoelectric sensor technique has been proven to yield reliable results in the laboratory. A number of papers by Zeng et al. have been published on the use of this technique [32].

1.4.1 History of the Piezoelectric Sensor

Pierre and Jacques Curie gave birth to the world of piezoelectricity. They were the first, in the year 1880, to demonstrate a connection between macroscopic piezoelectric phenomena and crystallographic structure. The experiment that demonstrated this connection consisted of specially prepared crystals such as tourmaline, quartz, topaz, cane sugar, and Rochelle salt which were subjected to mechanical stress. An irrefutable measurement of surface charges appeared on these crystals. In essence the crystals became electrically polarized. If one of these voltage-generating crystals was exposed to an electric field it lengthened or shortened (in tension and compression) according to the polarity of the field, and in proportion to the strength of the field. At the time, this phenomenon was regarded as a huge breakthrough, and was quickly termed "piezoelectricity", from the Greek word "piezen", meaning to press or squeeze. In 1881 the "converse effect" was mathematically deduced from fundamental thermodynamic principles [15]. More specifically, it was determined that not only did the crystals exhibit a direct piezoelectric effect (electricity from applied stress), but they also exhibit the converse effect (stress in response to applied electric field).

During the span from 1882 to 1917 the heart of "piezoelectric applications science" was launched. This included, "the identification of piezoelectric crystals on the basis of asymmetric crystal structure, the reversible exchange of electrical and mechanical energy, and the usefulness of thermodynamics in quantifying complex relationships among mechanical, thermal, and electrical variables" [15]. In 1910, a benchmark was reached when Voigt's "Lerbuch der Kristallphysik" was published. This became the standard reference work embodying the understanding of the framework underlying piezoelectricity.

However, the first developmental work on the application of piezoelectric devices did not take place until World War I in 1917. It was during this time that Langevin and French co-workers began to create and refine an ultrasonic submarine detector made of piezoelectric material [15]. More specifically, their

transducer was a medley of slender quartz crystals bonded between two steel plates. This device was secured and mounted in a watertight housing suitable for submersion. After the war's end, they ultimately achieved their goal of emitting a high frequency "chirp" underwater. Thus they were able to measure depth by timing the return echo.

The success of Langevin and his co-workers in the development of sonar began a shockwave of activity on many types of piezoelectric devices. Some of these devices and new ideas include megacycle quartz resonators (developed as frequency stabilizers for vacuum-tube oscillators), materials testing devices based on the propagation of ultrasonic waves, new ranges of transient pressure measurement devices that allowed for the study of explosives and internal combustion engines, microphones, accelerometers, signal filters, etc. Most of these classic piezoelectric applications were conjured up and implemented during the years following World War I (1920-1940).

During and after World War II (1940-1965), in the United States, Japan, and the Soviet Union, it was discovered that certain ceramic materials exhibited dielectric constants hundreds of times higher than common cut crystals. Not only that, but the composition, shape, and dimensions of the ceramics could be "cut-to-fit" the requirements of a specific application. Figure 1.9 shows some of the various "cut-to-fit" shapes created out of this material.
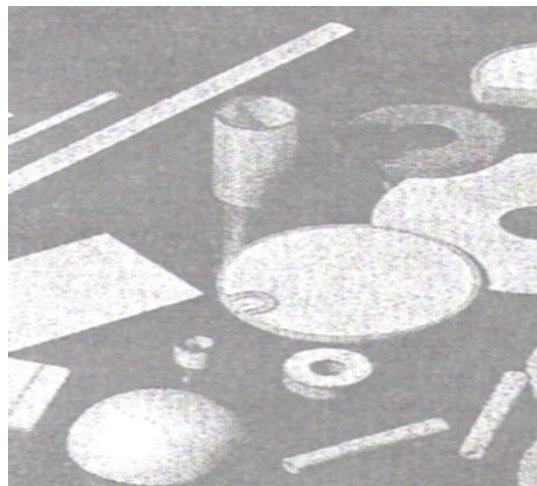

Figure 1.9   Various piezoceramic shapes.

These man-made piezoelectric materials soon replaced the natural materials in many applications as they are generally very physically strong, chemically inert, and are relatively inexpensive to manufacture. This discovery unsurprisingly began a resurgence of concentrated research and development of ceramic

devices. The advances in materials science that were made during this phase of discovery fall into three main categories [2]:

1. "Development of the barium titanate family of piezoceramics and later the lead zirconate titanate family."
2. "The development of an understanding of the correspondence of the perovskite crystal structure to electro-mechanical activity."
3. "The development of a rationale for doping both of these families with metallic impurities in order to achieve desired properties such as dielectric constant, stiffness, piezoelectric coupling coefficients, ease of poling, etc."

This progress contributed to the development of devices created by tailoring the ceramic material to work for a specific project. Powerful sonar, ceramic phonocartridge, piezo ignition systems, sonobouy, small sensitive microphones, ceramic audio tone transducers, relays, etc. were developed. The industry was soon dominated by the United States who secured a strong advantage with solid patents. However, it should be mentioned that during this time device development and piezo material development was conducted solely within individual companies. These companies held a "secrecy policy" and did not communicate due to the wartime research conditions. This was due to the fact that piezoceramic materials at the time were very difficult to develop, but extremely easy to replicate. With the secrecy policy enforced, the individual companies were driven by the thought of high profits controlled by solid patents. However, due to the competitive nature of this research, the market production for piezoelectric devices lagged behind the technical development by a very large margin. The growth of the industry soon became greatly impaired.

Japan shortly took advantage of the impaired industry and soon after, became the chief country in the development of knowledge, new applications, new processes, and commercial market areas. They did this by establishing a "competitively cooperative" association to oppose the United States' "secrecy policy." The goal of this association, which was later named the Barium Titanate Application Research Committee, was to set "an organizational precedent for successfully surmounting not only technical challenges and manufacturing complications, but also for defining new market areas" [15]. Through this association, Japan had taken charge in the development of piezoelectric devices.

Just as the development of these devices was regressing in the rest of the world, Japan's success became the spark that lit the fire. Many other nations began a new effort in the development of piezoelectric

products, which has continued today. Cutting edge technology is currently focused on "solid state motion." However, new original piezoceramic products are being developed daily.

1.4.2 The Structure of Piezoelectric Ceramics

Piezoelectric ceramic material generally consists of a group of perovskite crystals, individually consisting of a tiny, tetravalent metal ion, such as titanium or zirconium, surrounded by a lattice of larger, divalent metal ions, normally lead or barium, and O^{2-} ions. The general crystal structure can be thought of as a face centered cubic (FCC) lattice with a B^{4+} ion at the center surrounded by six O^{2-} ions, each at a face center, and eight A^{2+} ions, each at the corner (see Figure 1.10).

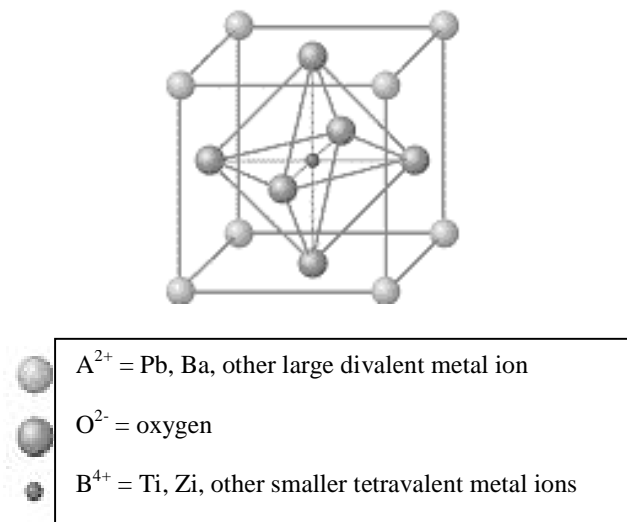| | A^{2+} = Pb, Ba, other large divalent metal ion |
| | O^{2-} = oxygen |
| | B^{4+} = Ti, Zi, other smaller tetravalent metal ions |

Figure 1.10   Crystal structure of a traditional piezoelectric ceramic [2].

To create a piezoelectric ceramic,

> "Fine powders of the component metal oxides are mixed in specific proportions, and then heated to form a uniform powder. The powder is mixed with an organic binder and is formed into structural elements having the desired shape (discs, rods, plates, etc.). The elements are fired according to a specific time and temperature program, during which the powder particles sinter and the material attains a dense crystalline structure. The elements are cooled, then shaped or trimmed to specifications, and electrodes are applied to the appropriate surfaces [2]."

At a specific temperature called the Curie temperature (named after Jacques and Pierre Curie) the crystal structure transforms from a non-symmetrical (tetragonal piezoelectric) to a symmetrical (cubic non-piezoelectric) form. At temperatures higher than the Curie point, each crystal element portrays a simple cubic symmetry with no dipole moment (Figure 1.11a). At temperatures lower than the Curie point, each crystal contains tetragonal or rhombohedral symmetry along with a dipole moment (Figure 1.11b). Adjoining diploes forming regions of local alignment are known as "domains." The alignment gives a net dipole moment to the domain, which in turn causes a net polarization. However, the direction of polarization among adjacent domains is random. This means that in essence, the ceramic element has no global polarization (Figure 1.12a).

Figure 1.11   **(a)** Cubic lattice, symmetric arrangement of positive and negative charges. **(b)** Tetragonal (orthorhombic) lattice, crystal has electric dipole [2].

The domains in a ceramic element can be aligned by exposing the element to a strong, direct current electric field (Figure 1.12b).

"Through this polarizing (poling) treatment, domains most nearly aligned with the electric field expand at the expense of domains that are not aligned with the field, and the element lengthens in the direction of the field. When the electric field is removed most of the dipoles are locked into a configuration of near alignment (Figure 1.12c). The element now has a permanent polarization, the remanent polarization, and is permanently elongated [2]."
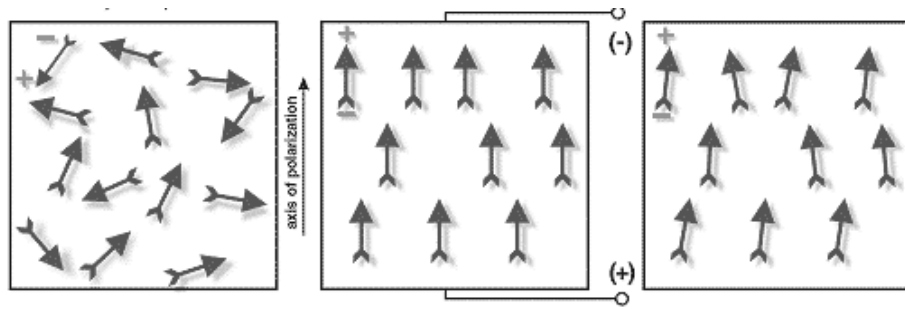
Figure 1.12 **(a)** Random orientation of polar domains prior to polarization. **(b)** Polarization in DC electric field. **(c)** Remanent polarization after electric field removed [2].

The number of domains that become aligned depends upon many variables. These include the poling voltage, temperature, and the amount of time the voltage is held on the material. During polarization the material permanently increases in dimension between the poling electrodes and decreases in dimensions parallel to the electrodes. The material can be de-poled by reversing the poling voltage, increasing the temperature beyond the material's Curie point, or by inducing a large mechanical stress.

1.4.3 Stability of Piezoelectric Ceramic Elements

Most properties of piezoelectric ceramics are not permanent and will gradually diminish over a period of time. A logarithmic relationship with time has been developed to represent the degradation of the ceramic element after the time at which it was initially polarized. The equation is as follows [2]:

$$\text{Rate of Aging} = (Par_2 - Par_1) / (Par_1 (\log t_2 - \log t_1))$$

Where, t_1 is the time one after polarization in days, t_2 is the time two after polarization in days, Par_1 is a value for the parameter Par at t_1, and Par_2 is a value for the parameter Par at t_2. However, the exact rate of aging is dependant upon the composition of the ceramic and the process used to manufacture the element.

It has been observed that ceramics age at two different rates. Within the first 24 to 50 hours after the polarization of the element, piezoelectric properties are rapidly lost. After this short period, the degradation of the ceramic occurs at a much slower rate throughout the lifetime of the element. The rate of aging can be increased by mishandling the elements in such a way that they could potentially be depolarized. This includes exceeding the electrical, mechanical, or thermal limitations of the element itself.

The following graph shows that for a particular element, the initial aging rate (for capacitance) 1,000 to 4,000 minutes after polarization is approximately -2.4% per decade. Following this initial period an aging rate of -0.9% was approximated per decade from then on.
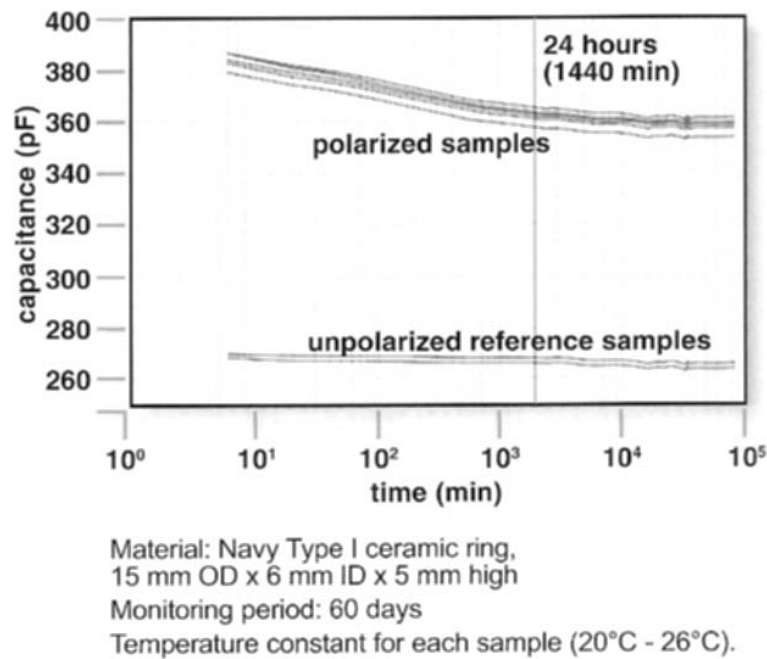

Material: Navy Type I ceramic ring,
15 mm OD x 6 mm ID x 5 mm high
Monitoring period: 60 days
Temperature constant for each sample (20°C - 26°C).

Figure 1.13 Capacitance loss after polarization [2].

1.4.4   Functioning of Piezoelectric Sensors

There are many different shapes and sizes of piezoelectric sensors, each created for a specific application. Amazingly enough, each different sensor functions in the same general fashion. Piezo motors, known as "actuators," convert electrical energy to mechanical energy. Piezo generators, known as "sensors," perform in an opposing fashion, converting mechanical energy into electrical energy. All piezo transducers (which convert one form of energy to another) can either exist as single sheets or two-layer elements. Single sheets can produce motion in any direction (thickness, length, and width directions) by a small excitation. These sheets produce electrical output when stretched or compressed. Two-layer elements are more resourceful and can be used in a multipurpose fashion. They can be treated as single sheets made up of two layers or they can be used to bend (bender elements) or extend (extender elements). Although they are called out as "two-layer," these elements actually consist of nine layers as shown in Figure 1.14. The layers of a two-layer element include four electrode layers followed by two piezoceramic layers bonded with two adhesive layers all strengthened by a center shim.
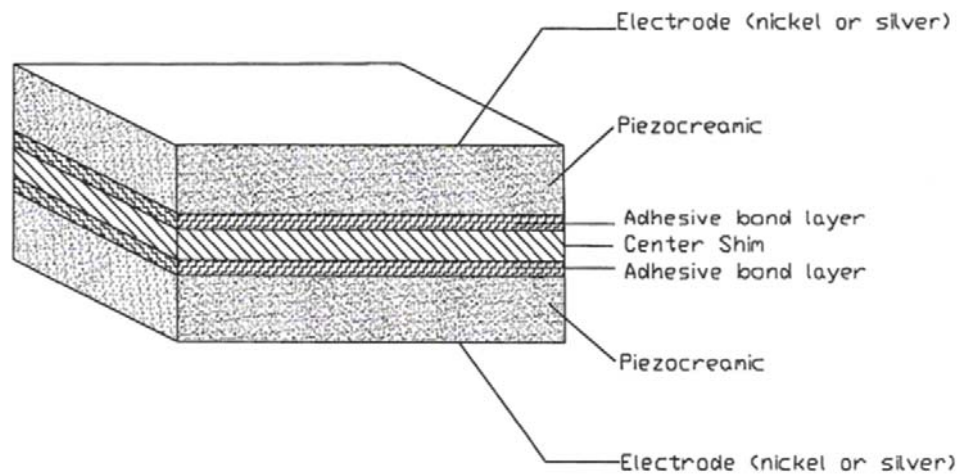
23

Figure 1.14   Various layers of a typical "two-layer" element.

The piezoceramic bender element is made up of two slender piezoceramic plates (sheets) which are inflexibly bonded together with conducting surfaces between them and on the outsides [12]. Because of the specific polarization of each plate a driving voltage applied to the element causes one plate to elongate and the other plate to shorten. This causes the element as a whole to bend, which means that one layer will go into tension while the other goes into compression. An electrical signal is the result of this phenomenon, which can be measured through the wire leads to the element. Figure 1.15 shows the bending displacement caused by an applied driving voltage.
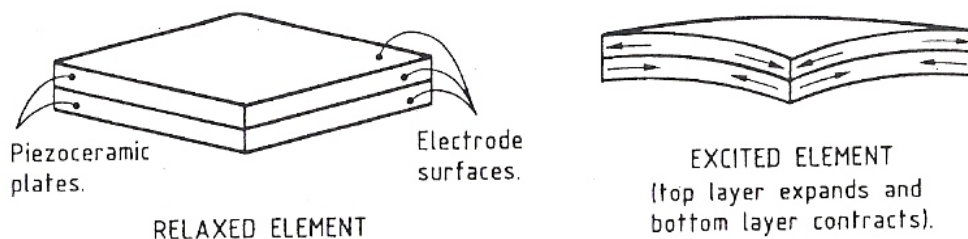

Figure 1.15   Shape of piezoceramic bender elements with and without applied excitation voltage.
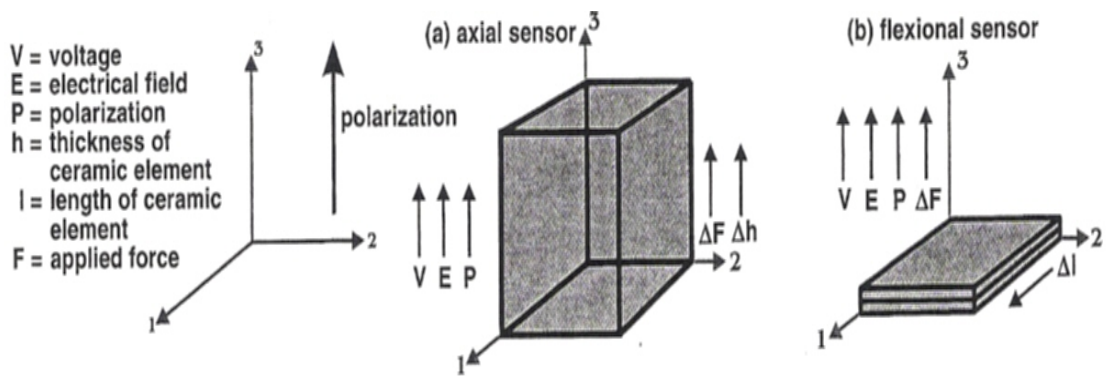
1.4.5 Piezo Generators (Sensors)

Figure 1.16 Relationship between mechanical input and electrical signal output by sensors [2].

Piezoelectric sensors are used in a fashion that converts force and motion to voltage and charge. There are two different types of sensors known as axial sensors and flexional sensors (refer to Figure 1.16). When a force is applied to a sheet of piezoceramic in a direction parallel to polarization a voltage is produced. This voltage attempts to return the piece to its original thickness (Figure 1.17a). This type of application involves the use of axial sensors. In the same fashion, when a force is applied to a sheet in a direction perpendicular to the polarization, a voltage is created which attempts to return the piece to its original length and width (Figure 1.17b). A single sheet fixed to a structural member which is deformed in some fashion will stimulate an electrical output.
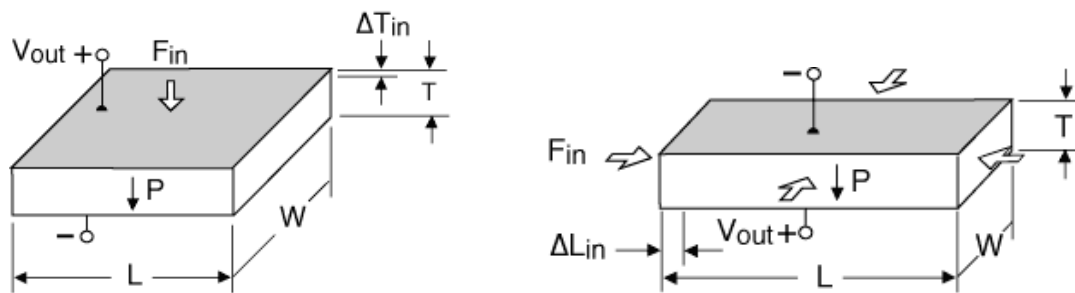

Figure 1.17 **(a)** Longitudinal generator. **(b)** Transverse generator.

Flexional sensors which are more common than axial sensors consist of two strips of piezoceramic bonded together to form a bilaminar element. Bender and extender elements are forms of flexional sensors. Usually these elements are fixed at one end and free on the other end where the input to be measured will act. This is known as a cantilever mounting system. An extension generator is created by bonding two single sheets of piezoceramic in such a way that an applied mechanical stress results in

electrical generation. The applied force causes both layers to deform in a similar fashion and a voltage is created which in turn tries to restore the element's original configuration. As described in Section 1.4.4, a bending generator operates in a similar mode. However, in this case each layer of the two-layer element deforms in an opposing fashion. One layer is compressed and the other layer is stretched. The following Figure 1.18 depicts a bending generator while Table 1.3 provides the common mode of vibration.
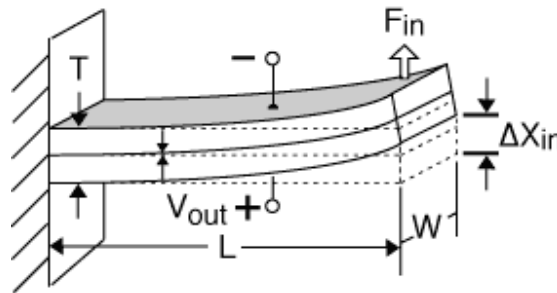

Figure 1.18   Bending generator of cantilever mount.

Table 1.3   Common mode of vibration for piezoceramic plate bender.

(Axis)	(Polarization Direction)	(Applied Field: Voltage Output)	(Mode of Vibration: Displacement)

Piezoceramic sensors work well with dynamic inputs as opposed to static inputs. They work extremely well as strain gauges in the determination of dynamic strains in structures.   In fact, the use of piezoceramics as strain gauges results in signal/noise ratios on the order of 50 times that of wire strain gauges.

1.4.6   Application in Soil Property Determination

The ability to tailor a material to a specific application makes the use of piezoceramic sensors very attractive to the world of geotechnical engineering. Many experimental techniques have been recently introduced employing bender and extender elements for the determination of soil properties.   The

procedure used is quite simple. An electrical excitation is applied to a transmitter element which leads to mechanical vibrations and in turn generates shear (s) waves (for a bender element). In a similar fashion, primary (p) waves are produced by extender elements. The s- and p-waves produced by the transmitter elements then result in an electrical output produced by receiving elements. The velocity of the s- and p-waves can then be determined by measuring travel time and distance between the wave transmitter and receiver. This technique has been successfully used by a number of researchers including Dyvik and Madshus in 1985, Thomann and Hryciw in 1990, Jovicic in 1996, Viggiani and Atkinson in 1995, Hryciw and Thomann in 1993, Jovicic and Coop in 1998, and Zeng and Ni in 1998 and 1999 to measure the stiffness of sands and clays in the laboratory.

Zeng describes several equations used to determine soil properties employing bender and extender elements as follows [32]:

Assuming that the distance between an s-wave transmitter and an s-wave receiver is L_s and the time for the wave to travel this set distance is t_s, the average shear wave velocity can be calculated as,

$$V_s = L_s / t_s$$

Correspondingly for the velocity of the p-waves,

$$V_p = L_p / t_p$$

Where L_p is the distance between the extender element transmitter and receiver and t_p is the travel time of the p-wave. The shear modulus of the soil, G_{max}, can be calculated as,

$$G_{max} = \rho * V_s^2$$

Where ρ is the mass density of the soil. The constrained modulus of the soil is then,

$$M = \rho * V_p^2$$

The Poisson's ratio (μ) is represented by,

$$\mu = [(M / G_{max} - 2) / (2M / G_{max} - 2)]$$

Finally, the elastic modulus can be determined using,

$$E = 2G_{max} * (1 + \mu)$$

1.4.7   Proposal for a New Testing Device

In the geotechnical laboratory at Case Western Reserve University, a new field testing technique has recently been developed. This technique is used to measure the stiffness and Poisson's ratio of soils using cone penetrometers equipped with piezoelectric sensors (Figure 1.19).
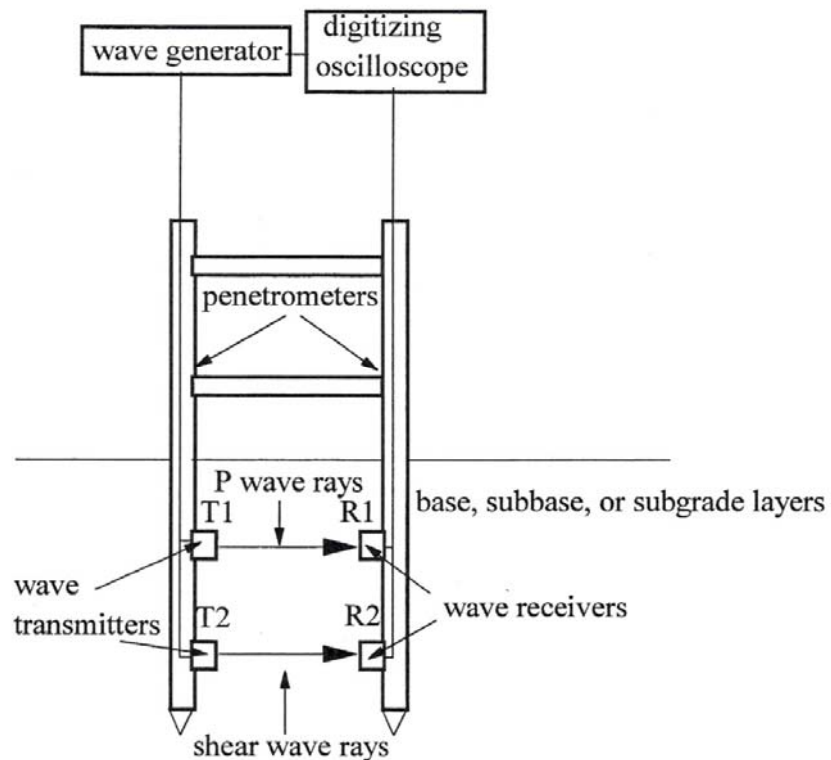

Figure 1.19   Cone penetrometer equipped with piezoelectric sensors.

A pair of cone penetrometers is fitted with two sets of piezoelectric sensors (one set of bender elements and one set of extender elements as described in Section 1.4.6). The idea of using the penetrometers is that they can easily be pushed into foundation soils (Figure 1.20a and 1.20b). One set of the sensors is used as wave transmitters while the other set is used as wave receivers as shown in Figure 1.19. A function generator is used to produce an electrical pulse which in turn activates the transmitters. Primary and shear waves are created by the vibration of the transmitters. These waves propagate

through the soil and are captured by the receivers. Then, from the measured velocities of shear and primary waves soil stiffness and Poisson's ratio can be determined using the equations of Section 1.4.6. Thus far, this technique has been proven to produce reliable results in the laboratory [32].
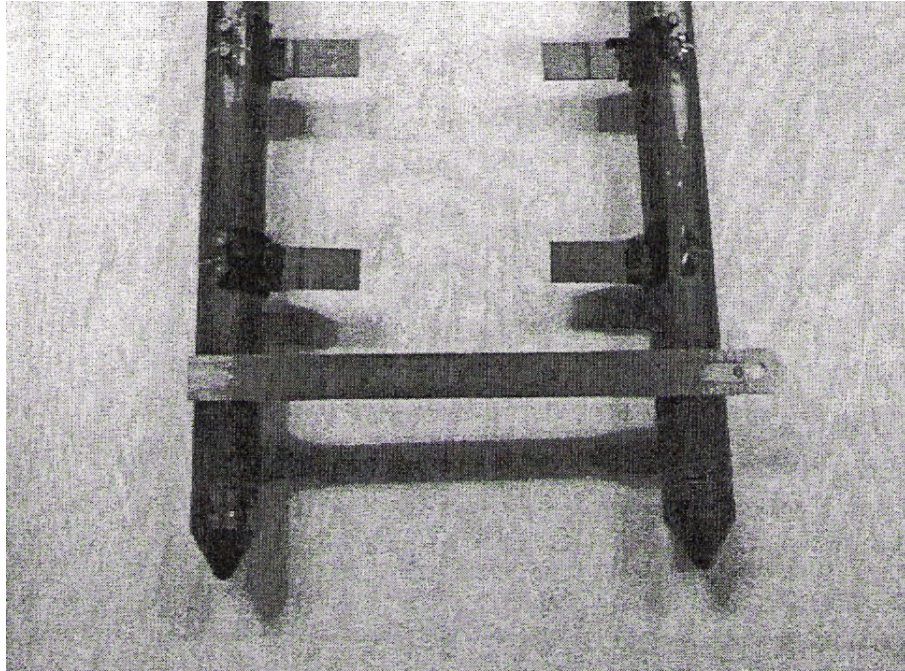

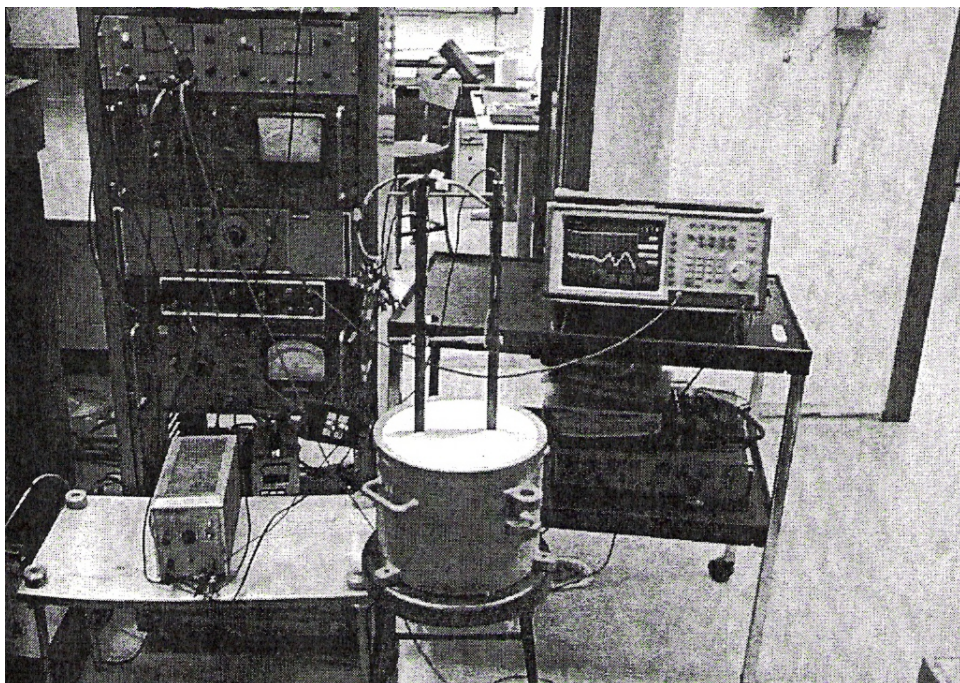**Figure 1.20(a)**   Cone penetrometer equipped with piezoelectric sensors [20].

Figure 1.20(b)   CPT laboratory setup [20].

The goal of this thesis is to delve further into the development of the cone penetrometer with piezoelectric sensors and to produce a low cost, automated and mobile unit that can be widely used during highway construction for monitoring and controlling construction quality of highway pavements and for evaluating performance of existing pavements. In addition, the system shall be versatile, user friendly, and applicable to all types of soils and field conditions.

1.5   Organization of the Report

This thesis presents the development, experimentation, results, and conclusions of the field-testing technique incorporating cone penetrometers equipped with piezoelectric sensors for the measurement of soils stiffness in highway pavements. While Chapter One was a brief introduction to the material, Chapter Two contains a literature review of materials covering the usage of bender-extender element techniques for the measurement of soil properties. Chapter Three includes a detailed description of the development of this field-ready device, including the experimental setup and a summary of testing procedures. Chapter Four outlines and summarizes the results of the testing. Finally, Chapter Five provides a general conclusion, closure to the thesis, and suggestions for further research in this subject area.

CHAPTER TWO
LITERATURE REVIEW

2.1   Review of Piezoelectric Sensors in Measuring Soil Properties

Geologists and seismologists were among the first to study elastic waves in granular materials in order to better understand the behavior of seismic waves in the loose materials comprising the earth's crust. In 1939, a researcher named Iida studied compression and torsional shear wave velocity in granular materials [21]. Gassman and Brandt then advanced the theoretical work begun by Iida. In their studies, they included both uniform packings of like spheres and random mixtures of different spheres. Previously in 1950, Paterson showed that unlike a classical solid material that could only support a dilatational and a shear wave disturbance, porous granular materials could support three waves: a dilatational wave through both the mineral skeleton and through the pore fluid, and a third, shear wave, through the mineral skeleton. Following Paterson's work, in 1962, Biot proposed a comprehensive theory relating all three disturbances. He pointed out that the frame wave speed must be influenced by the presence of the pore fluid and cannot solely reflect the properties of the mineral skeleton.

Piezoelectric crystals were first introduced as one of two methods used at this time as a means to measure elastic wave velocities in the laboratory. The first method was introduced by Ishimoto and Iida in 1936.

> "The method consists of vibrating one end of a cylindrical sample at various frequencies, until the frequency which gives maximum response is found. This frequency is the resonant frequency of the sample. If the mode of vibration is known the wave length may be determined from the height of the sample, and the relation,

$$c = f * \lambda$$

> Where f, the frequency of the response and λ, the wavelength, may be used to calculate the wave velocity (c) [21]."

The second method involving piezoelectric ceramics consists of initiating a shear wave at one point within a sample and detecting its arrival at a second point. If the distance between the two points is

known, the velocity characteristic of the disturbance can be calculated directly from the required transit time using the formula where distance equals rate times time. Paterson in 1956, Lawton in 1957, and Lawrence in 1963 were among the first to employ this technique [21]. This technique is generally more attractive than the resonant column method due to the fact that it only requires very minute disturbances (5.75×10^{-16} cm or 10^{-6} inches) as compared to the 6.92×10^{-11} cm (10^{-4} inches) required by the latter method. Thus, the pulse technique is, in essence, the more successful form of non-destructive testing.

The first major experiment performed by Lawrence using piezoelectric crystals occurred in 1963 and was conducted on two granular materials including Ottawa sand and spherical glass beads [22]. The equipment used in the study consisted of an electronic pulse generator, a pair of barium titanate piezoelectric transducers, and an oscilloscope capable of observing both the voltages impressed on the sending transducer and the voltage resulting from the arrival of the stress pulse in the receiving transducer. The goal of using this type of transducer was to produce waves of minimum amplitude which would not affect the basic "soil fabric." In other words, it would remain well within the elastic range of the material. Piezoelectric crystals were the then obvious choice for producing these high frequency elastic waves of small amplitude.

> "The experimental technique consisted of measuring the time delay between the voltage impressed on the sending transducer and the voltage from the receiving transducer (Figure 2.1). From the delay time and the measured separation of the crystal faces, the velocity of the propagation of the stress wave was computed. With this apparatus, the shape of the received wave forms and their characteristic frequencies were also observed [20]."
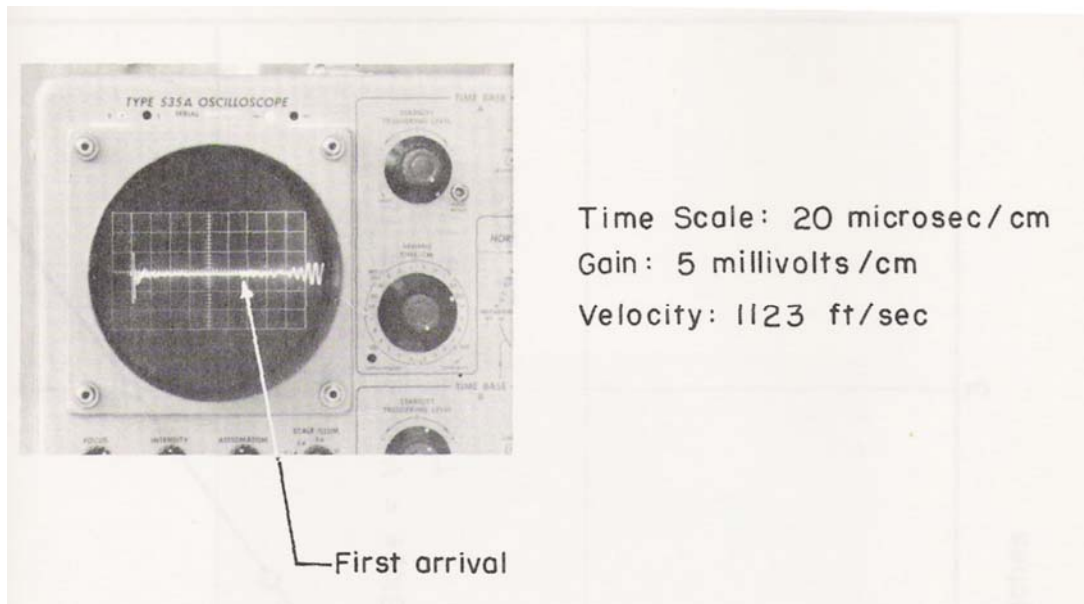
Time Scale: 20 microsec/cm

Gain: 5 millivolts/cm

Velocity: 1123 ft/sec

—First arrival

Figure 2.1   First arrival of shear wave.

In conclusion to this study on non-saturated granular systems, it was determined that measurements of dilatational wave speed taken by the pulse method proved satisfactory. However, using these low sensitivity crystal receivers, difficulty was experienced in clearly determining the first elastic-wave arrival.

Soon after, several other complications were discovered in using this type of crystal transducer, the main difficulty being an opposition between the characteristic impedance of the crystal element and that of a soil specimen [12]. More simply put, "The mechanical motion that is transferred to the soil is small because the element exhibits a small movement with a large force and the soil exhibits a large movement with a small force [23]." The problem with these elements was overcome with the development of piezoceramic bender bimorph elements for use as shear-wave generators and receivers, developed by Shirley and Anderson and Shirley and Bell in 1977. This element is composed of two crystals bonded together in a sandwich-type arrangement. It is essentially a plate element which juts into the soil specimen in a cantilevered fashion. In general, the element is assembled in such a fashion that when a voltage is applied to the electrodes, the crystal will deform in opposite directions causing the bimorph to bend as described in Section 1.4.4. The bimorph bends side to side displacing the soil in a direction perpendicular to the length of the element. A considerable coupling factor is created with the soil. In turn, a shear wave is produced which promulgates perpendicular to the motion of the soil particles. The displacement created by a bimorph element is much greater than that of the single crystal as used in Lawrence's experiment in 1963. This element was successfully used by Shirley to measure the shear wave velocity in kaolinite clay.

33

In 1980, Dominic F. Howarth used ultrasonic piezoelectric transducers in a triaxial cell in fundamental studies investigating the mechanical properties of rock and the effect of rock fabric/texture on these properties [16]. In general, he developed equipment enabling the determination of the dynamic Young's modulus of triaxially loaded rock cores.

In 1981, Strachan studied the relationship between liquefaction resistance and shear and fluid wave velocities using bender elements and compressive disks secured in triaxial cell end caps. In this experiment, samples could be subjected to dynamic loads after measuring the elastic-wave behavior [10]. The equipment used in this experiment involved the use of bender elements projecting directly into the soil sample. This type of setup was apparently suitable for laboratory purposes, but could not be used in-situ. Strachan also noted that problems and possible damage to the benders themselves developed when bender motion was inhibited by high effective stresses. Shultheiss and Hamdi and Taylor Smith in 1981 and 1982, respectively, have also successfully used bender elements mounted in various laboratory apparatus to measure the shear wave velocity in a soil specimen.

DeAlba [10] conducted liquefaction tests in 1984, using a cyclic triaxial device equipped with piezoelectric bender elements. The tests conducted were used to confirm an immediate relationship between liquefaction resistance and shear or compressive wave velocities in saturated sand. Six characteristically different sands were tested and results showed that relationships between elastic-wave velocities and liquefaction resistance could indeed be established for each material. These results allowed for the conclusion that in-situ measurements of elastic-wave velocities can be used to recreate laboratory samples to their field liquefaction resistance. It should be noted that simple measurements of elastic-wave velocities alone will not put a figure on liquefaction resistance, since the resistance-velocity relationship is also material dependent.

As can be seen, bender elements have historically been installed and used in an assortment of traditional geotechnical laboratory testing equipment. Not only have they been included in triaxial testing, but they have also been useful in direct simple shear and oedometer devices [12]. From this, several significant advantages have been created in that:

> "The quality of each individual specimen in these different tests can be evaluated, the
> need to run parallel resonant column tests is eliminated, G_{max} and the other geotechnical
> parameters from the test (i.e. shear modulus at large strains from triaxial or shear) can be

determined and compared for the same specimen, and G_{max} measurements can be a useful guide during consolidation (i.e. to determine the rate of application of the drained deviator stress in an anisotropically consolidated triaxial test). The only disadvantage of these new techniques is that there is no direct or convenient method to determine the dampening ratio of the soil and G at high strain levels [12]."

In 1985, Dyvik and Madshus installed bender elements in the Drnevich resonant column device (Hardin oscillator) at NGI. Their goal was to take G_{max} measurements simultaneously by both methods (bender elements and resonant column) on the same soil sample and compare the results. Figure 2.2 depicts the setup for integrating bender elements in the resonant column device. Tests were performed on three different offshore clays, a sample of Drammen clay and a specimen of Haga clay.
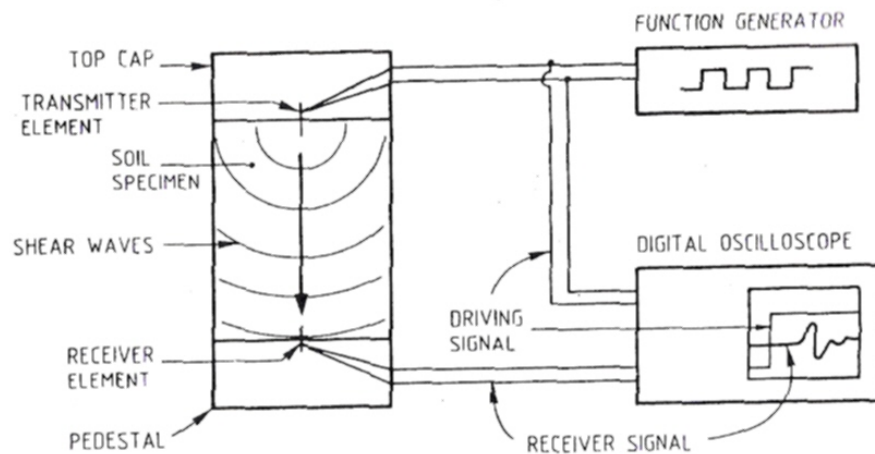

Figure 2.2   Setup for the integration of bender elements in the resonant column apparatus [12].

The outcome as shown by Figure 2.3 encompasses a vast array of soil G_{max} values. Generally, the two different techniques concur. As can be seen from the graph, the best results are at a stiffness value of approximately 75 MPa (10.9 kip/in^2). "Although the resonant column technique is a well established method for determining G_{max} in the laboratory, there is nothing that says these results are exactly correct, so these two techniques actually serve as a check on each other" [19]. One simple advantage of using the bender element over the resonant column method is that the test procedures and computations for bender elements are much easier.
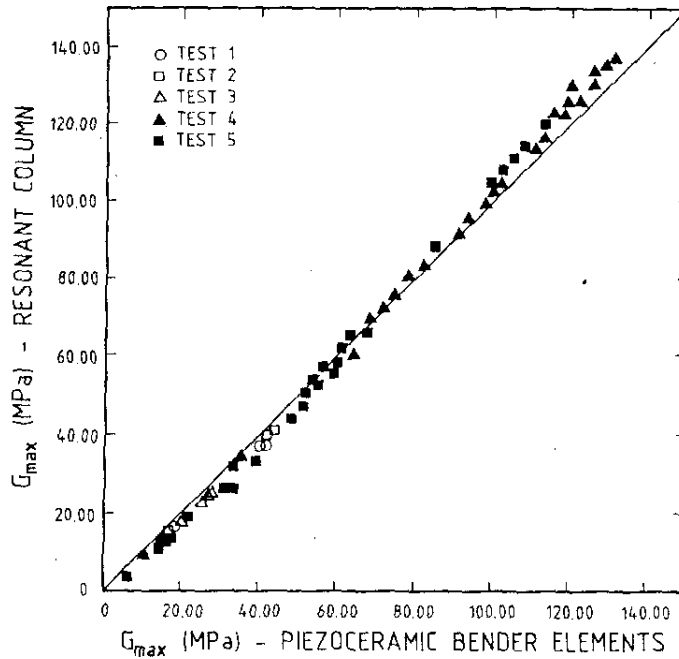
Figure 2.3 G_{max} results.

In 1990, Thomas Thomann and Roman Hryciw presented a new laboratory device capable of measuring the small strain shear modulus under a no lateral strain (K_o) condition. Measurement of shear wave velocity, as previously mentioned, is ordinarily performed in a resonant column device under isotropic confinement. This presents a problem though, as soils in the field are usually under a K_o condition during vertical loading, unloading, and reloading. Thus, the vertical and horizontal stresses in-situ are going to be quite different from the isotropic conditions created in resonant column testing. The new testing device is comparable to an oedometer and utilizes bender elements to measure the shear wave velocity (see Figure 2.4 below). The device can also be used to determine the effects of aging and secondary consolidation. This is due to the fact that the change in void ratio can be measured more accurately than in a standard resonant column device. The following figure shows the bender element-oedometer (BEO) device setup as proposed by Thomann and Hryciw.
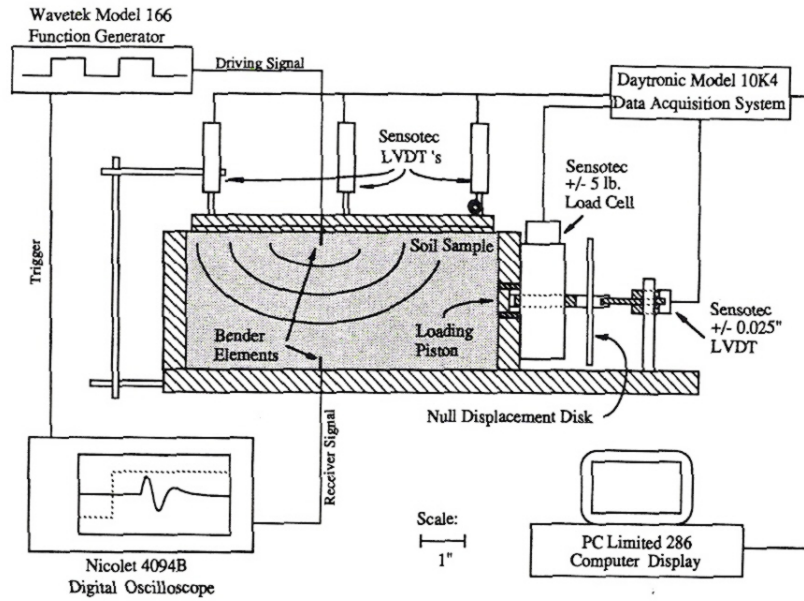
36

Figure 2.4   Bender element-oedometer [29].

A compilation of tests on Ottawa sand were executed to assess the performance of this BEO device. The results of the testing eventually indicated that the device is capable of successfully measuring the lateral stresses and the shear wave velocity under K_o conditions.

In 1998, Zeng and Ni developed a new application of bender elements to measure the small strain shear modulus of sand in four different shear planes under anisotropic loading conditions [34]. Then in 1999, Zeng and Ni applied the bender element technique to investigate the stress-induced anisotropy in G_{max} of sands. The general focus of the work follows a basic study of the technique itself, a hypothetical framework for stress induced anisotropic G_{max} of sand and its authentication by experimental data. Along with this new technique, an empirical equation to determine the K_o of sand was suggested and verified by test results [35].

In 2001, Lings and Greening created a single "crossbreed" element called the "bender-extender" element. This element can transmit and receive both shear (s) and primary (p) waves using a single pair of elements. These elements were mounted and tested using a dry sand sample. A 10 kHz 20 VPP (volt peak to peak) sine wave was used as the impulse signal. Results showed that the received bender-extender signals were clear and concise.

2.1.1 Common Problems Related to the Bender Element Technique

In a bender element test the most common problems are related to the determination of shear wave travel time. Shear wave velocity is calculated using the distance and travel time of shear waves between the ends of a transmitter and a receiver. In essence, distance equals rate multiplied by time. The distance can be measured quite accurately using a simple ruler or tape measure, but the most difficult part is the determination of the wave travel time from the transmitter to the receiver. The travel time of shear waves in a bender element test as defined by Zeng is,

"The time interval between the instant when a transmitter initiates vibration and the time when the shear waves reach a receiver. Generally speaking, the initial vibration of a transmitter is considered to take place at the instant when an electrical signal is applied, whereas the arrival of shear waves at a receiver is taken as the instant when an electrical output is recorded from the receiver. However, finite element analysis shows that there exists a phase lag between the electrical signal and the initial vibration of a transmitter [35]."

In addition, there can be great difficulty in determining the arrival time of the shear wave when interference is created by other waves. This topic has been the investigation of several more current studies performed by Boulanger in 1998, Viggiani and Atkinson in 1995, and Jovicic in 1996. It has been shown that a great disturbance is created when other waves arrive before the shear wave itself. There can also be problems even when the shear wave arrives first. This is due in part to the strength of the signal. In both cases according to Zeng, "The first arrival of the shear wave is masked so that an accurate determination of the arrival of shear waves is not possible [35]." The problem in these experiments is the ability to positively determine the arrival of the s-wave. In 1981, Abbiss suggested that this be accomplished by using a source which is rich in s-waves [1]. In addition, the polarity of the s-waves can be reversed thus reversing the signal produced on the seismograph trace and positively identifying the shear wave arrival (see Figure 2.5).
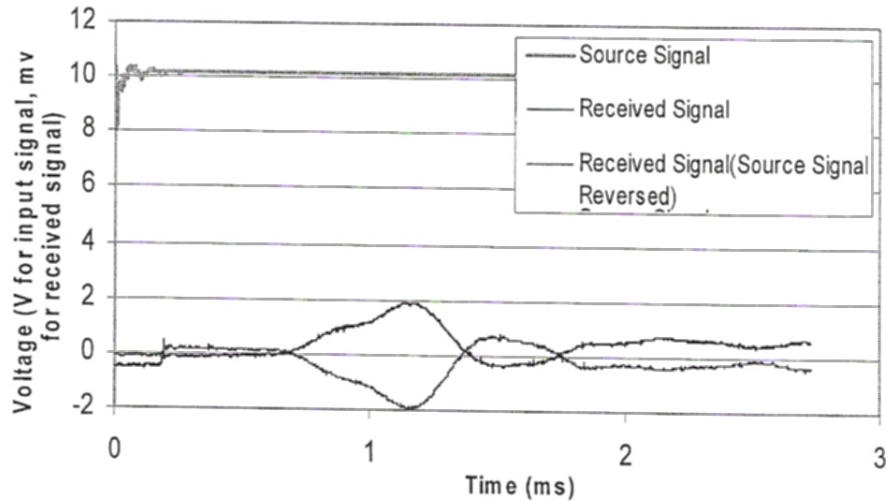
Figure 2.5   Reversed signal for s-wave.

Another factor affecting bender element test results lies in the rising time (T_r) of the source signal. Zeng and Ni discovered in their 1999 experimental explorations that when the rising time is increased, the maximum electrical output from the receiver can be appreciably diminished. To study the effect of rising time on test results, Zeng and Ni placed a receiver approximately 2.5 centimeters (cm) away from a transmitter and used three different electrical pulses as input signals. The results showed that the change in rise time was independent of the travel time for shear waves. However, the definition of the first arrival seemed to be affected by the size of the T_r. If the rising time was too large, the vibration of the transmitter was too weak causing a poorly defined shear wave. Therefore it was determined that, a square pulse can only be used as the input signal for bender element tests in the situation that the rising time is small.

The size of bender elements plays a large role in the strength of the signal acknowledged by a receiver. In cases of high stress levels, the movement of a bender element is greatly impeded and cannot vibrate at a strong enough intensity to produce a strong signal for the receiver to pick up. Therefore, the sizes of transmitters and receivers need to be determined to measure accurately the shear-wave velocity at high stresses. Generally speaking, the intensity of the vibration of a bender element increases as its size and flexibility increase. According to Zeng and Ni, "The size plays a more important role for a transmitter, whereas it is the flexibility that is important for a receiver [35]."

2.2   Measuring Stiffness and Poisson's Ratio Using Piezoelectric Sensors

In recent years several testing methods have been born, which measure the stiffness properties (including elastic modulus, shear modulus, and Poisson's ratio) of soils. These measurements are utilized in the design of highway pavements and in quality control / quality assurance processes. Consequently, organizations such as AASHTO, ODOT, and the NCHRP have dedicated various funds and research projects toward the investigation of these properties. Throughout the highway community the major pavement design emphasis is now on rehabilitation, for which, as has been previously stated, empirical design approaches have become inadequate. The overwhelming recommendation for improvement to this approach seems to lie within the basis of new mechanistic principles and design methods supported by historic empirical methods. With this recommendation comes the exploration and development of new testing devices and data interpretation algorithms.

2.2.1   Stiffness Testing

At present, the most popular technique to determine the stiffness of underlying highway pavement soils is to conduct a California Bearing Ratio (CBR) test. This test is specifically used on soil samples prepared in the laboratory. The resulting value (or CBR) is then applied to calculate the resilient modulus of soils, M_R, using compatible empirical expressions. One expression recommended by AASHTO is as follows,

$$M_R = 10,340 * CBR \text{ (kPa)}$$

The use of the resilient modulus was developed and proposed by the Strategic Highway Research Program in 1987. Several other methods had previously been used, but failed according to the FHWA's standards. In 1996, The Federal Highway Administration (FHWA) issued a new standard protocol for M_R testing called the "Long Term Pavement Performance Protocol P46." This LTPP program protocol describes, "the laboratory preparation and testing procedures for the determination of the Resilient Modulus of unbound granular base and subbase materials and subgrade soils under specified conditions representing stress states beneath flexible and rigid pavements subjected to moving wheel loads" [30]. The value of resilient modulus determined from this protocol procedure is a measure of the elastic modulus of unbound base and subbase materials and subgrade soils recognizing certain nonlinear characteristics. This protocol became very popular in the late 1990's and was recently improved upon

with the new 2002 NCHRP 1-28A protocol. The advantages of the new protocol include more clear definitions of material classification and the applied stress and time duration are more representative to the field conditions [24].

However, there are still a number of limitations for this method. As mentioned previously, the majority of the testing methods use samples of the base, subbase, and subgrade layers that have been prepared and compacted in the laboratory using procedures that are very different from what the soils are subjected to in-situ. The laboratory compacted specimens may possibly have stiffnesses different from the soils compacted in the field. Secondly, these tests do not offer the specific pieces of information needed by engineers and pavement designers to establish whether the stiffness of pavement materials and soils under construction (in the field) meet the design constraints. In addition, for an existing pavement where the subgrade, subbase, and the base soils have experienced years of weathering and traffic loading applications, the current testing methods are not capable of determining the stiffness of these in-situ soils. Finally, the value of Poisson's ratio is an extremely valuable consideration in pavement design calculations. Currently, the value of Poisson's ratio is being estimated rather than measured in most design cases [32]. Therefore, there is the need to develop a new testing method for the measurement of stiffness and Poisson's ratio of the soils.

CHAPTER THREE

DEVELOPMENT OF CONE PENETROMETER WITH PIEZOELECTRIC SENSORS AND TESTING PROCEDURE

3.1 Need For New Testing Equipment

In recognition of the new highway construction guide proposed by the American Association for State Highway and Transportation Officials and the final report for NCHRP 1-37A new testing developments for stiffness of the underlying soils/materials of highway pavements are rapidly being proposed. Current testing methods are becoming out-dated and the employment of strictly empirical methods has been pushed away. Non-destructive, in-situ, mechanistic testing and design approaches are the new "fad" in the world of highway engineering.

In this chapter, a new non-destructive testing device is presented. This new device is based on the design of the cone penetrometer recently developed by Dr. Zeng in the Case Western Reserve laboratory. It is intended to accurately and quickly measure the shear modulus, constrained modulus, Young's modulus, and Poisson's ratio of the underlying soils of highway pavements during and after construction. The basic design employs two cone penetrometers equipped with one set of bender elements and one set of extender elements. The penetrometers can be pushed into the ground with the assistance of an ultrasonic vibratory hammer (if needed) and the soil parameters can easily be determined. The use of an ultrasonic vibratory hammer will provide minimal disturbance to the soil structure itself as the penetrometer is being pushed into the ground. With this device the future of pavement engineering will be greatly improved.

3.2 Basic Piezo-Cone Penetrometer Structure

The initial design of the piezo-cone penetrometer is shown in the following Figures 3.1 and 3.2. It consists of one set of bender elements, one set of extender elements (for a total of four piezoelectric sensors), two rectangular push rods, two solid removable cones, and one adjustable connection/extension rod. The push rods themselves each consist of two pieces of .64 cm x 5.08 cm x 30.48 cm (¼" x 2" x 12") flat stock stainless steel fixed with 12 screws. This material is a lightweight, durable, and rustproof material extremely suitable for field conditions. Two rectangular areas for the bender and extender elements were milled in the steel as well as an area to place and protect the lead wires (see Figure 3.3). The cone tips are also fabricated from stainless steel and are removable as they

simply screw into the base of the rods. If the cones get dull or damaged for any reason they can easily be replaced or repaired. The penetrometers themselves are connected to each other with a horizontally adjustable connection/extension rod. The rod is held in place by a set screw which can be adjusted to provide differing lengths between the elements for optimum performance. The elements themselves can also be horizontally adjusted for maximum performance or maximum protection (see Figure 3.4).
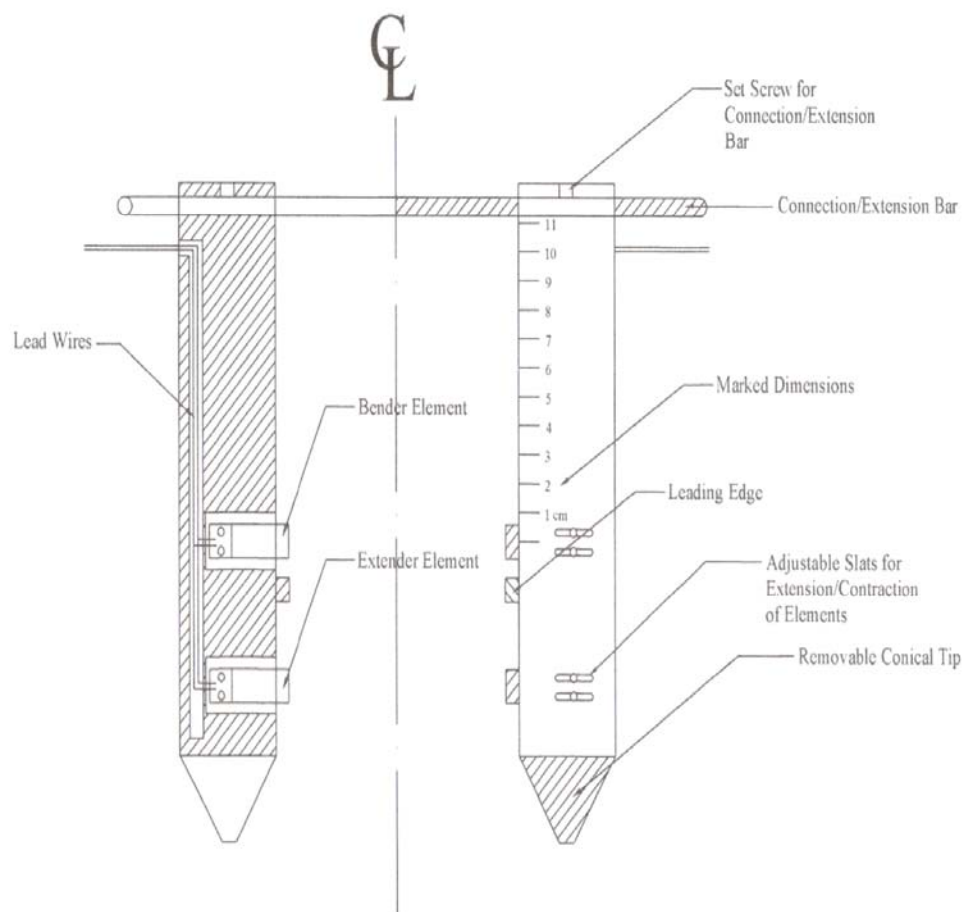

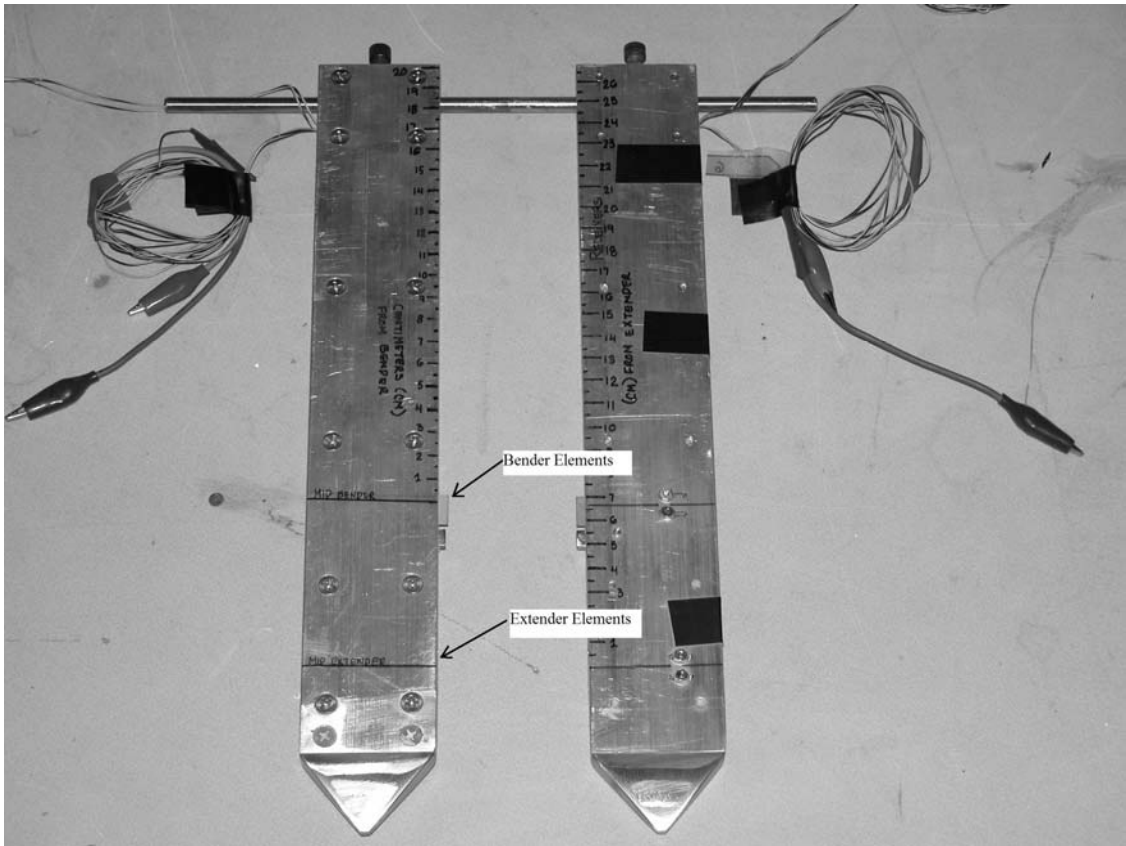**Figure 3.1**   Piezo-Cone Penetrometer schematic.

Figure 3.2   Photograph of the new Piezo-Cone Penetrometer.

Figure 3.3   Photograph of the milled areas for the elements.
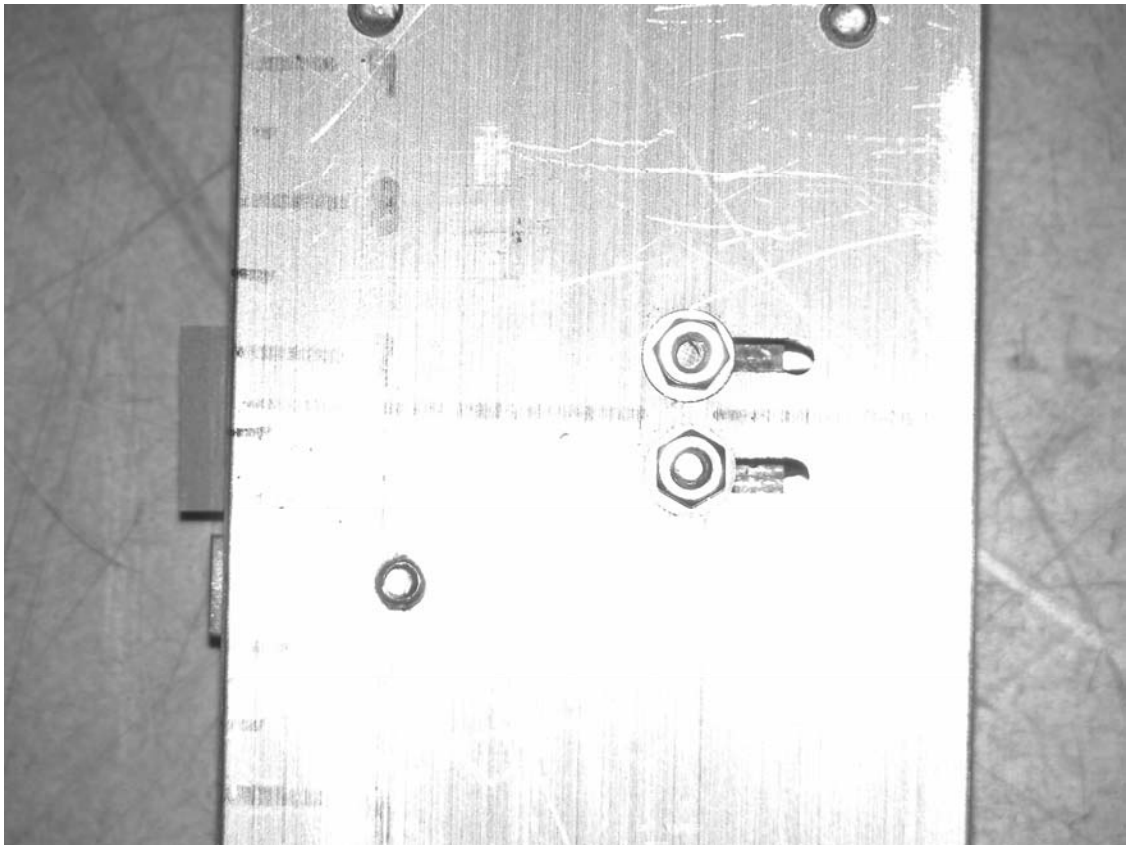
Figure 3.4   Adjustable slats for bender and extender elements.

The piezoelectric sensors employed in this design were purchased from Piezo Systems Inc. of Cambridge Massachusetts (as shown in Figure 3.5). Bender element type Q220-A4-303Y (transmitter) and type Q220-A4-303X (receiver) were used in the cone penetrometer. Extender element Q220-A4-303YE (transmitter) and element Q220-A4-303XE (receiver) were used in the cone penetrometer as well.
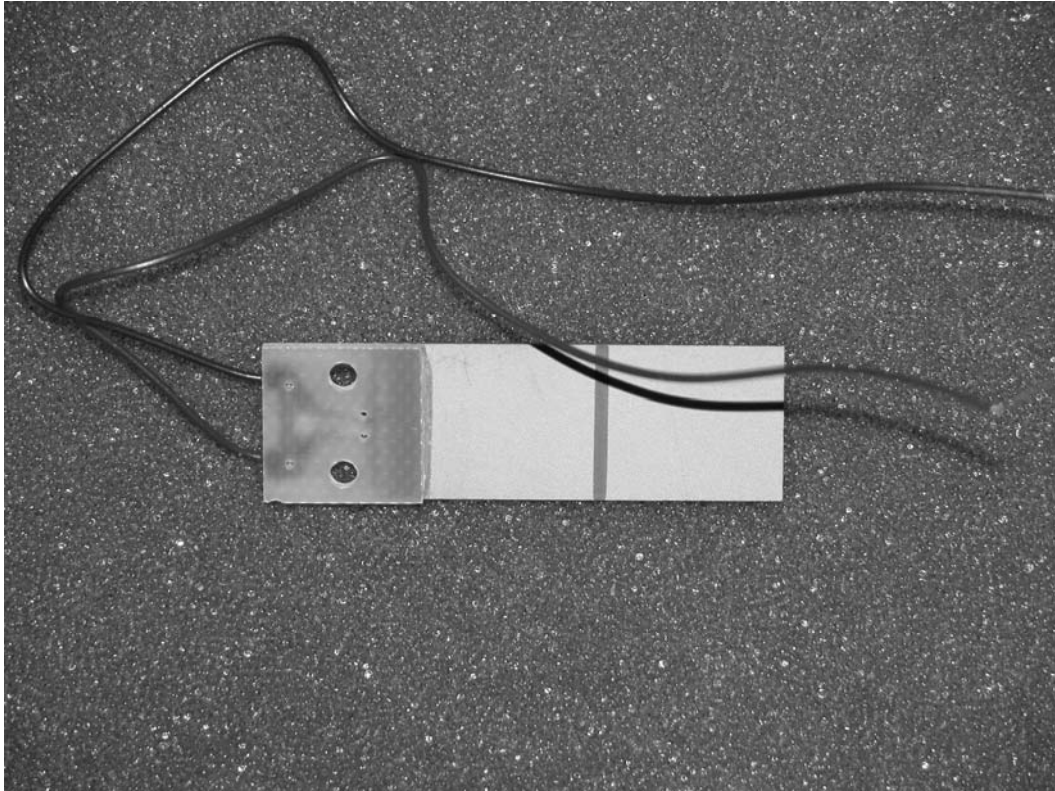
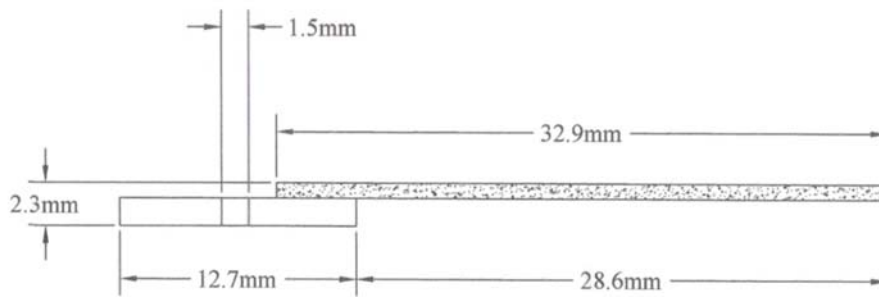**Figure 3.5** Piezoceramic element from Piezo Systems, Inc.
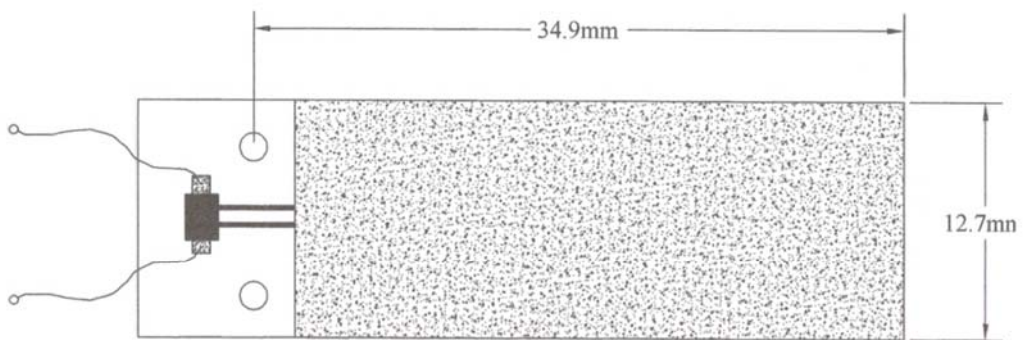
Figure 3.6   Bender and extender element dimensions.

Each sensor can be coated with an epoxy which creates a watertight seal and protects the sensors from any possible abrasions incurred while pushing the rods into the foundation material. Any electrical connections (wires, etc.) can be sealed with a waterproof coating as well, but will be well protected as they are fixed inside the cone penetrometers themselves.

3.3   Soil Description

Two different types of sand were used in the testing of this device to simulate soil materials that may be found underlying highway pavements. Nevada sand was one of the sands used for the testing of this device. It was purchased from the Gordon Sand Company of Compton, California and has a grain size distribution as shown in the following diagram (Figure 3.7(a)). Common index properties of Nevada sand are shown in the following Table 3.1(a).
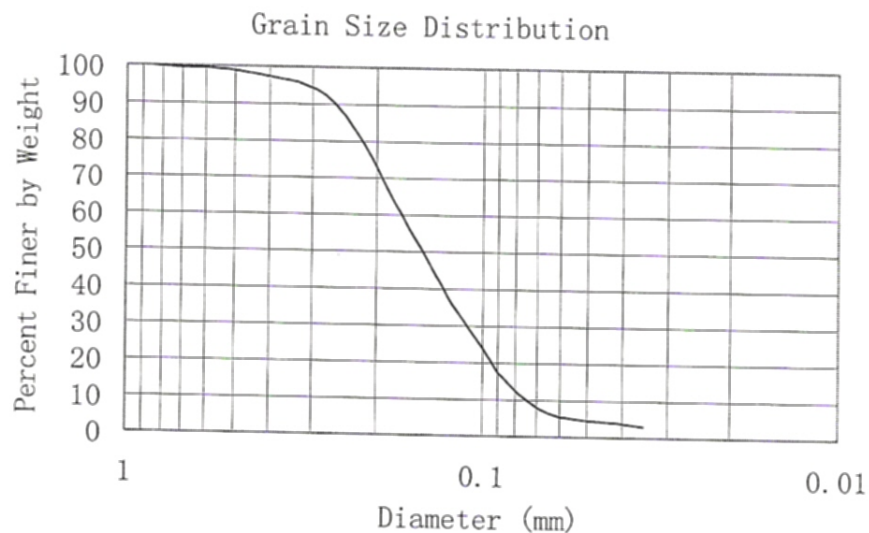
Figure 3.7(a)   Grain size distribution for Nevada sand.

Table 3.1(a)   Index Properties of Nevada Sand

Parameter	Value
D_{50}	0.17 mm (0.007 in)
D_{10}	0.09 mm (0.004 in)
C_U	2
C_C	1
Specific Gravity	2.67
Maximum Dry Density	17.33 kN/m^3
Minimum Dry Density	13.87 kN/m^3
Maximum Void Ratio	0.887
Minimum Void Ratio	0.551

The other sand used in the testing of this device was a mixture of different sands found in the laboratory at Case Western Reserve University. The grain size distribution is shown in the following diagram (Figure 3.7(b)) and the index properties are provided in the accompanying table (Table 3.1(b)). This sand was a much coarser-grained sand than the Nevada sand and can be classified as well-graded whereas the Nevada sand is classified as a poorly-graded sand.

Grain Size Distribution
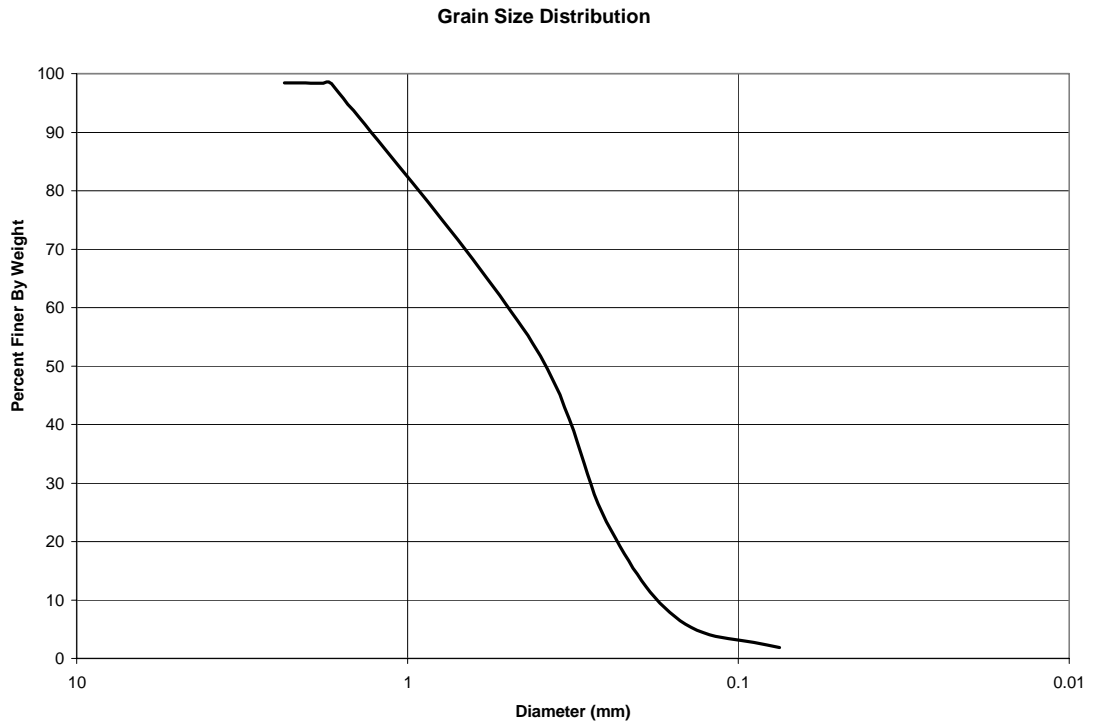
Figure 3.7(b)   Grain size distribution for coarser-grained mix sand.

Table 3.1(b)   Index properties of coarser-grained mix sand.

Parameter	Value
D_{50}	0.36 mm (0.014 in)
D_{10}	0.18 mm (0.007 in)
C_U	1.9
C_C	0.5

3.4   Experimental Setup

The experimental setup for the laboratory testing of the piezo-cone penetrometer is shown in the following Figure 3.8. A 33120A Agilent Waveform Generator was used to produce the triggering source signals. A square impulse wave was used as the source signal versus a regular sine wave. Square waves have been known to produce clearer and more reliable results. A 54624A Agilent Oscilloscope was used to capture and display the received signals and a 467A Hewlett Packard Power Amplifier was used to increase the intensity of the images captured by the oscilloscope to aid in a clear reception of the received signals.

Figure 3.8   Experimental setup for laboratory tests.

3.4.1   Theory Behind the Testing

The shear wave velocity and the shear modulus can be calculated from the travel time of the shear waves produced and received between the top set of bender elements. In this situation, the following equations are employed:

$$V_s = L_s/t_s$$
$$G_{max} = \rho * V_s^{\,2}$$

In a similar fashion the primary wave velocity and the constrained modulus can be calculated from the travel time of the primary waves produced and received between the bottom set of extender elements. In this case, the following equations are employed:

$$V_p = L_p/t_p$$
$$M = \rho * V_p^{\,2}$$

50

Using the calculated values for the shear modulus and the constrained modulus taken at the same depth, the Poisson's ratio can be calculated as:

$$\mu = [(M/G_{max} - 2)/(2*M/G_{max} - 2)]$$

Finally, the elastic modulus can also be calculated as:

$$E = 2*G_{max}(1 + \mu)$$

3.4.2   Laboratory Test Procedure

Laboratory tests were conducted on the two different soil specimens described above. The samples were prepared in a steel container with a diameter of 29 centimeters (11.4 inches) and an overall height of 40 cm (15.7 in). The steel container had enough lateral stiffness to simulate a K_o condition that is characteristic of conditions found in the field. Too often different analyses assume that soils have isotropic properties which lead to significant errors in the calculation of soil properties. Imposing a K_o condition in the laboratory creates anisotropic soil properties which are representative of those usually existent in the field. Soil samples were created by pouring the sands into the container using a hopper. In the creation of each sample, the height and rate of pouring were kept constant so as to achieve uniformity throughout the soil sample. Four different samples were prepared (two Nevada sand samples and two coarse-grained sand samples). A loose sample and a dense sample of each type of sand were created by varying the height of the hopper (the greater the distance between the hopper and the container, the more dense the sample, vice versa). The sands were poured to a height of 31.5 cm (12.4 in). After each sample was prepared, the penetrometer was gently pushed into the soil until the piezoelectric sensors reached a specified depth (see Figure 3.9). Bender and extender element tests were then conducted to measure the s- and p-wave velocities. After recording these measurements, the cone penetrometer was pushed to deeper positions in the soil to obtain other measurements. Upon the final depth of testing, the s-wave velocities, p-wave velocities, shear modulus, constrained modulus, and the elastic modulus were calculated. The sample container used in the laboratory limited the measurement of the soil parameters to a depth of approximately 15 centimeters (5.9 in). For tests conducted in the field, deeper sections of subgrade can be characterized, but in the laboratory the depth was restricted by the height of the container. In addition, measurements of s- and p-wave velocities were taken at the same locations (however not at the same time) in order to calculate Poisson's ratio for the corresponding

depth. To ensure repeatability of the data, each test was conducted on a second sample prepared in the same fashion and excellent repeatability of the results was obtained.
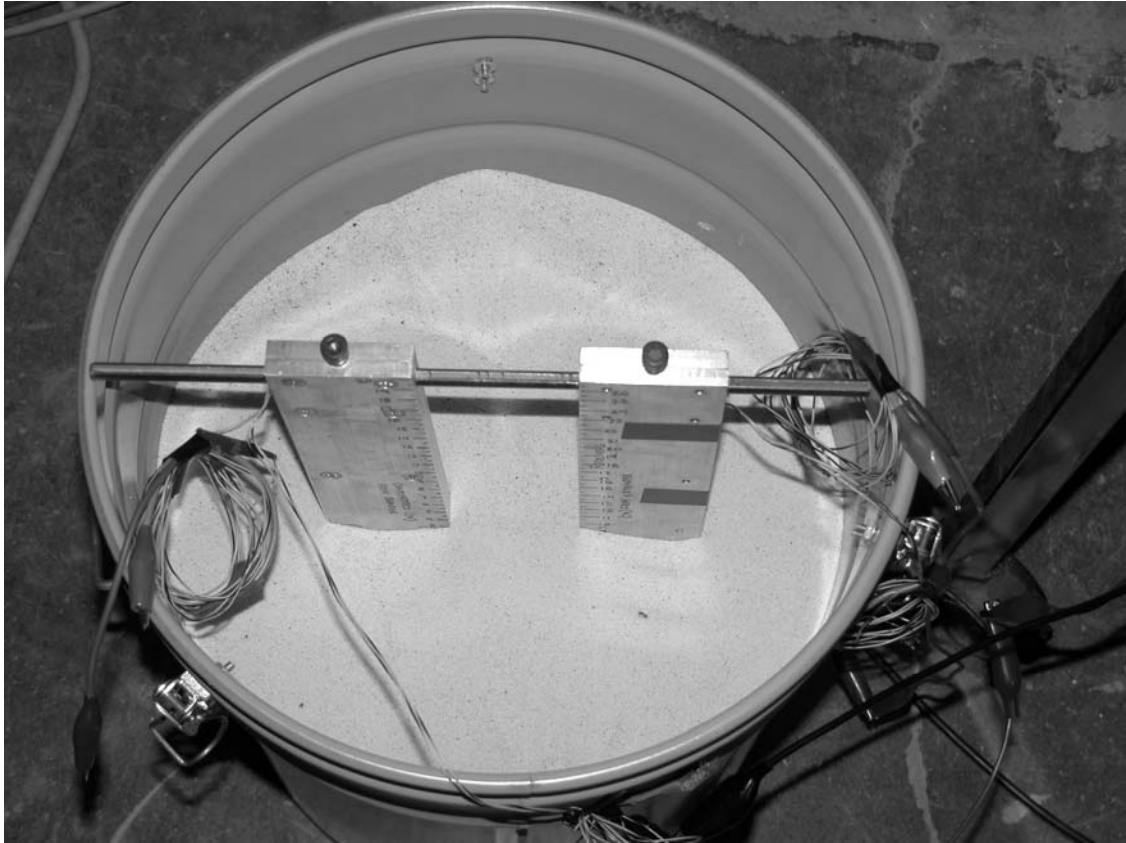
Figure 3.9   Penetrometers are pushed into the sand to a specified depth.

Field tests can be preformed in a similar fashion. The piezo-cone penetrometer can be pushed directly into the sublayers of a pavement under construction. A vibratory hammer can be used in cases where stiffer soils do not allow the penetrometer to be easily pushed into the ground. For an existing pavement, two holes can be cored through the upper layers of asphalt and the penetrometers again can be gently pushed into the underlying soils. The testing procedure and calculations described above can then be implemented at different depths to obtain and check the mechanical properties of the soil sublayers. Since this test is considered a non-destructive test, very little disturbance to the under layers of new or existing pavements is created. Thus, results are likely to be reliable and accurate.

CHAPTER FOUR
REVIEW AND DISCUSSION OF TESTING RESULTS

4.1 Test Overview

Figure 4.1a and 4.1b are typical waves recorded by the oscilloscope for the bender and extender element (respectively) test results. The wave-time is recorded where the beginning of the s- or p-waves first appear. In most test cases, the arrival point of the wave was very clear and concise. In cases where the arrival point was not clear, the signal was repeated at varying durations until it became more clearly identifiable. Generally a frequency of around 210 to 250 Hz produced waves of the clearest form.
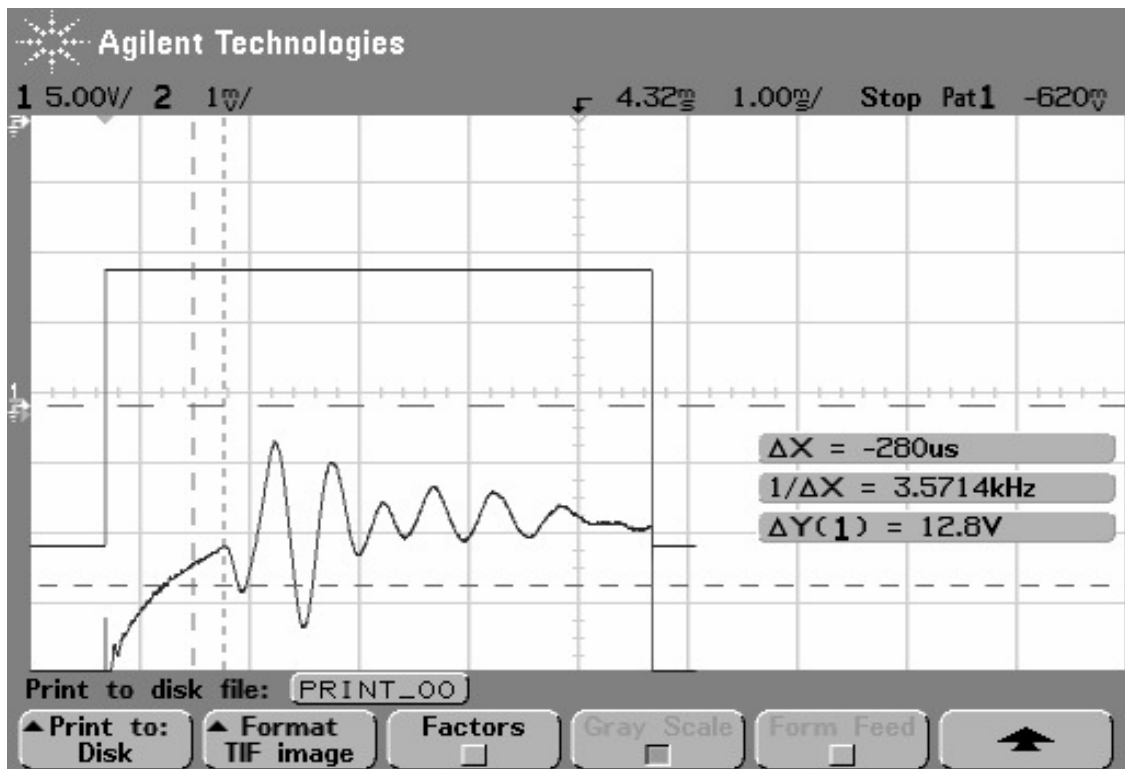
Figure 4.1(a)   Typical s-wave recording.
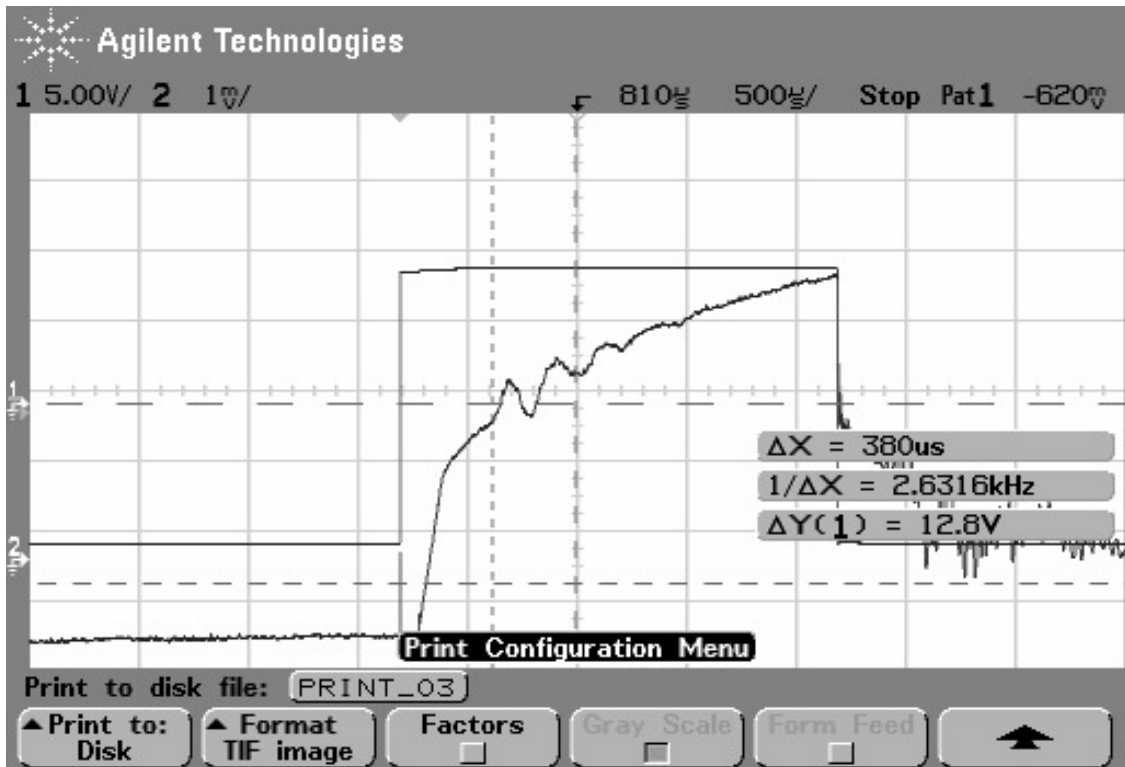
Figure 4.1(b)   Typical p-wave recording.

4.2   Sample Calculation

The following calculations were used in the assessment of the data collected by the piezo-cone penetrometer tests. This data is drawn from the results for the loose Nevada sand sample taken at a depth of 13 cm (5.1 in) with a mass density of approximately 1,452 kg/m^3 (0.05 lb/in^3).

The wave speeds can be calculated as:

$$V_s = L_s/t_s$$
$$V_s = (5 \text{ cm} / 720 \text{ μs}) * 10,000 = 69.4 \text{ m/s (155.2 mph)}$$

And,

$$V_p = L_p/t_p$$
$$V_p = (5.4 \text{ cm} / 420 \text{ μs}) * 10,000 = 128.57 \text{ m/s (287.6 mph)}$$

The shear modulus can be calculated as:

$$G_{max} = \rho*V_s^2$$
$$G_{max} = 1,452 \text{ kg/m}^3 * (69.4 \text{ m/s})^2 * 0.000001 = 7.00 \text{ MPa (146.2 kip/ft}^2)$$

54

The constrained modulus can be calculated as:

$$M = \rho * V_p{}^2$$

$$M = 1{,}452 \text{ kg/m}^3 * (128.57 \text{ m/s})^2 * 0.000001 = 24.00 \text{ MPa } (501.3 \text{ kip/ft}^2)$$

Poisson's ratio is now calculated as:

$$\mu = [(M/G_{max} - 2) / (2*M/G_{max} - 2)]$$

$$\mu = [(24 \text{ MPa} / 7 \text{ MPa} - 2) / (2*24 \text{ MPa} / 7 \text{ MPa} - 2)] = 0.294$$

To compare the shear modulus from the test results Hardin and Richart's 1963 equation is solved as:

$$G_{max} = (2{,}630 * F(e) * \sigma'm^{0.5}) / 145.04$$

Where,

$$F(e) = (2.17\text{-e})^2 / (1\text{+e}) = 0.96$$

$$\sigma'_m = [(1+2*k_o)/3]*\sigma'_v*145.04 = 0.157 \text{ psi}$$

So,

$$G_{max} = (2{,}630 * 0.96 * 0.157^{0.5}) / 145.04 = 6.90 \text{ MPa } (144.1 \text{ kip/ft}^2)$$

4.3   Test Results

The following tables and graphs provide results for the four different tests conducted in the laboratory. For further reference, complete tables and graphs have been provided in Appendix A.

Table 4.1   Test results on loose Nevada sand.

Depth of Extender (cm)	Depth of Bender (cm)	Constrained Modulus (Mpa)	Max Shear Modulus (MPa)	Poisson's Ratio	H-R G_{max} (Mpa)
1 .39 in	1 .39 in	16.94 2456.9 psi	3.11 451.1 psi	0.3874	1.92 278.5 psi
3 1.18 in	3 1.18 in	16.94 2456.9 psi	4.48 649.8 psi	0.3201	3.32 481.5 psi
5 1.97 in	5 1.97 in	36.62 5311.3 psi	5.97 865.9 psi	0.4027	4.29 622.2 psi
7 2.76 in	7 2.76 in	26.46 3837.7 psi	4.91 712.1 psi	0.3861	5.07 735.3 psi
9 3.54 in	9 3.54 in	26.46 3837.7 psi	7.00 1015.3 psi	0.3201	5.75 833.9 psi
11 4.33 in	11 4.33 in	26.46 3837.7 psi	4.91 712.1 psi	0.3861	6.36 922.4 psi
13 5.12 in	13 5.12 in	24.00 3480.9 psi	7.00 1015.3 psi	0.2941	6.91 1002.2 psi
15 5.91 in	15 5.91 in	24.00 3480.9 psi	7.41 1074.7 psi	0.2768	7.43 1077.6 psi

Table 4.2   Test results on dense Nevada sand.

Depth of Extender (cm)	Depth of Bender (cm)	Constrained Modulus (Mpa)	Max Shear Modulus (Mpa)	Poisson's Ratio	H-R G_{max} (Mpa)
1 .39 in	1 .39 in	13.20 1914.5 psi	3.49 506.2 psi	0.3201	3.02 438.0 psi
3 1.18 in	3 1.18 in	19.79 2870.3 psi	3.92 568.5 psi	0.3767	5.23 758.5 psi
5 1.97 in	5 1.97 in	24.54 3559.2 psi	6.21 900.7 psi	0.3307	6.75 979.0 psi
7 2.76 in	7 2.76 in	20.62 2990.7 psi	6.21 900.7 psi	0.2846	7.99 1158.9 psi
9 3.54 in	9 3.54 in	29.70 4307.6 psi	5.77 836.9 psi	0.3793	9.06 1314.0 psi
11 4.33 in	11 4.33 in	29.70 4307.6 psi	7.05 1022.5 psi	0.3443	10.01 1451.8 psi
13 5.12 in	13 5.12 in	28.27 4100.2 psi	7.05 1022.5 psi	0.3338	10.88 1578.0 psi
15 5.91 in	15 5.91 in	32.91 4773.19 psi	10.60 1537.4 psi	0.2625	11.69 1695.5 psi

Table 4.3   Test results on loose coarse-grained sand.

Depth of Extender (cm)	Depth of Bender (cm)	Constrained Modulus (Mpa)	Max Shear Modulus (Mpa)	Poisson's Ratio	H-R G_{max} (Mpa)
1 .39 in	1 .39 in	15.22 2207.5 psi	2.62 380.0 psi	0.3959	1.70 246.6 psi
3 1.18 in	3 1.18 in	17.87 2591.8 psi	4.17 604.8 psi	0.3478	2.94 426.4 psi
5 1.97 in	5 1.97 in	25.73 3731.8 psi	4.56 661.4 psi	0.3924	3.79 549.7 psi
7 2.76 in	7 2.76 in	31.76 4606.4 psi	6.11 886.2 psi	0.3809	4.49 651.2 psi
9 3.54 in	9 3.54 in	23.33 3383.7 psi	4.36 632.4 psi	0.3852	5.09 738.2 psi
11 4.33 in	11 4.33 in	25.73 3731.8 psi	4.36 632.4 psi	0.3981	5.62 815.1 psi
13 5.12 in	13 5.12 in	35.61 5164.8 psi	8.10 1174.8 psi	0.3527	6.11 886.2 psi
15 5.91 in	15 5.91 in	35.61 5164.8 psi	9.80 1421.4 psi	0.3101	6.57 952.9 psi

Table 4.4   Test results on dense coarse-grained sand.

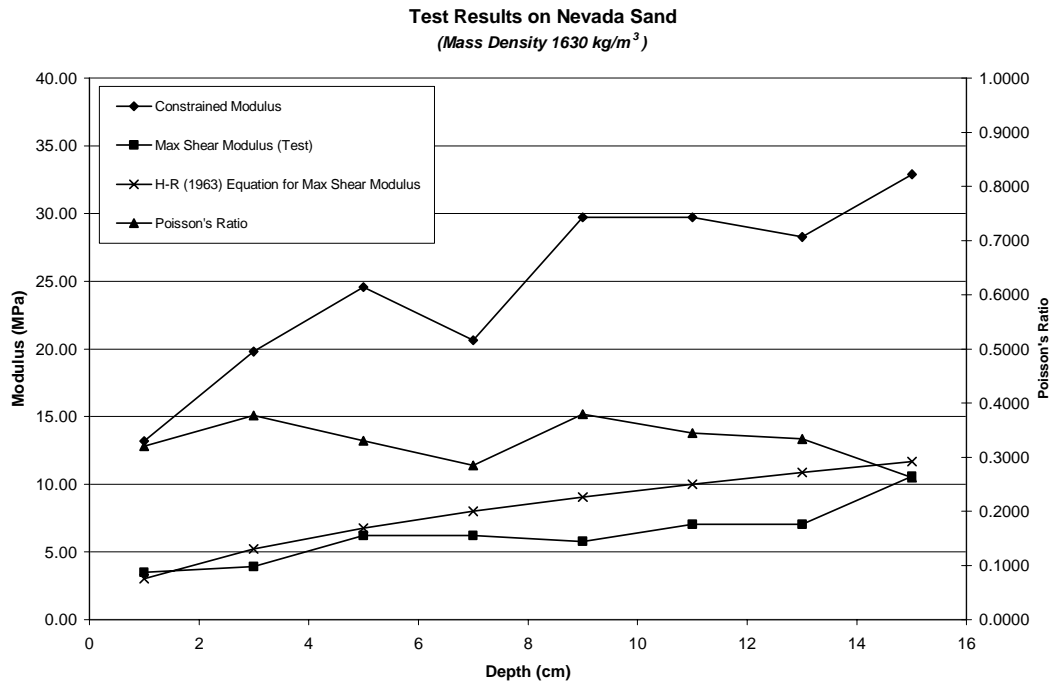| Depth of Extender (cm)	Depth of Bender (cm)	Constrained Modulus (Mpa)	Max Shear Modulus (MPa)	Poisson's Ratio	H-R G_{max} (Mpa)
1 .39 in	1 .39 in	12.63 1831.8 psi	3.11 451.1 psi	0.3368	2.56 371.3 psi
3 1.18 in	3 1.18 in	18.18 2636.8 psi	4.60 667.2 psi	0.3304	4.43 642.5 psi
5 1.97 in	5 1.97 in	31.48 4565.8 psi	5.80 841.2 psi	0.3872	5.72 829.6 psi
7 2.76 in	7 2.76 in	31.48 4565.8 psi	6.75 979.0 psi	0.3636	6.76 980.5 psi
9 3.54 in	9 3.54 in	28.41 4120.5 psi	7.12 1032.7 psi	0.3329	7.67 1112.4 psi
11 4.33 in	11 4.33 in	35.86 5201.1 psi	6.75 979.0 psi	0.3841	8.48 1229.9 psi
13 5.12 in	13 5.12 in	35.07 5086.5 psi	7.12 1032.7 psi	0.3727	9.22 1337.2 psi
15 5.91 in	15 5.91 in	44.39 6438.2 psi	7.95 1153.1 psi	0.3909	9.90 1435.9 psi

Test Results on Nevada Sand
(Mass Density 1452 kg/m^3)
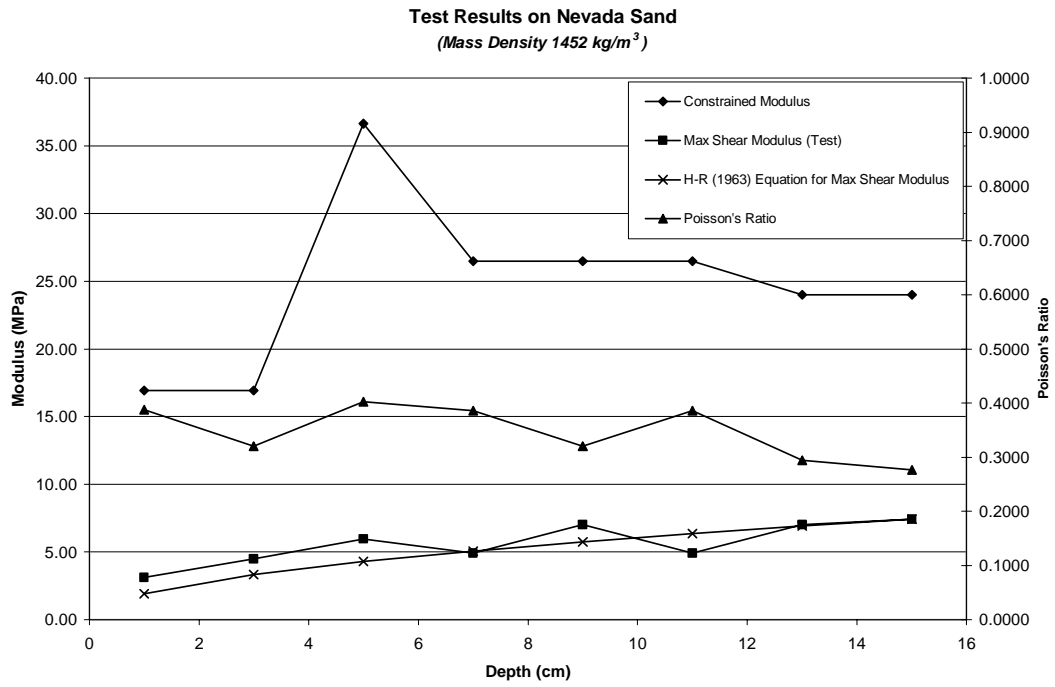
Figure 4.2   Test results on loose Nevada sand.

Test Results on Nevada Sand
(Mass Density 1630 kg/m^3)

Figure 4.3   Test results on dense Nevada sand.

Test Results on Mix Coarser-Grained Sand
(Mass Density 1412 kg/m³)
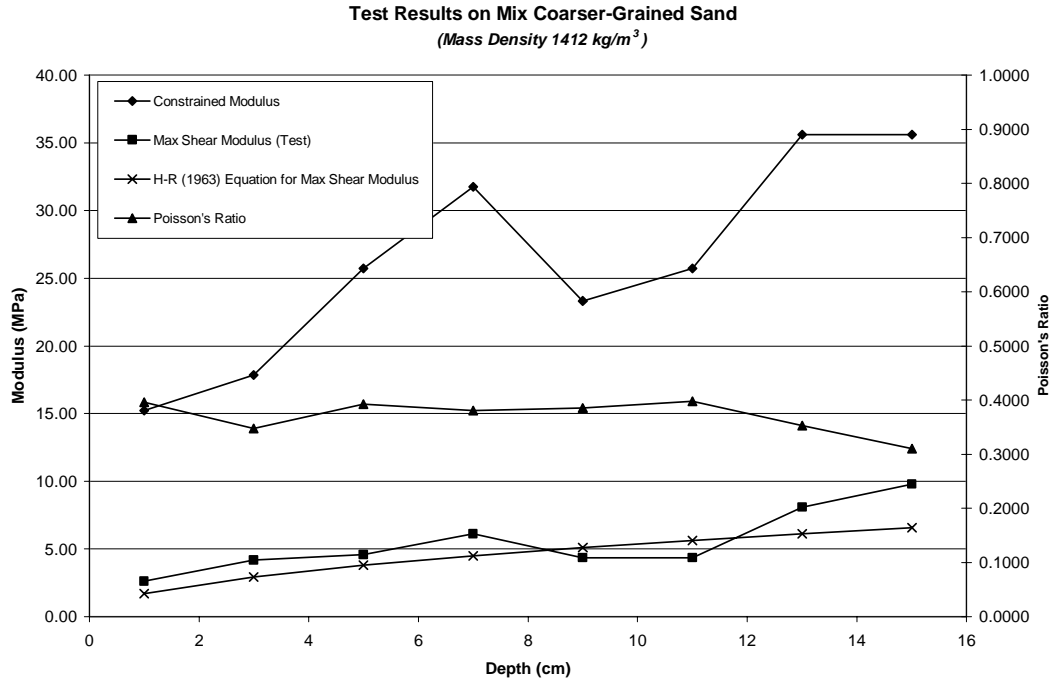
Figure 4.4   Test results on loose coarse-grained sand.

Test Results on Mix Coarser-Grained Sand
(Mass Density 1559 kg/m³)

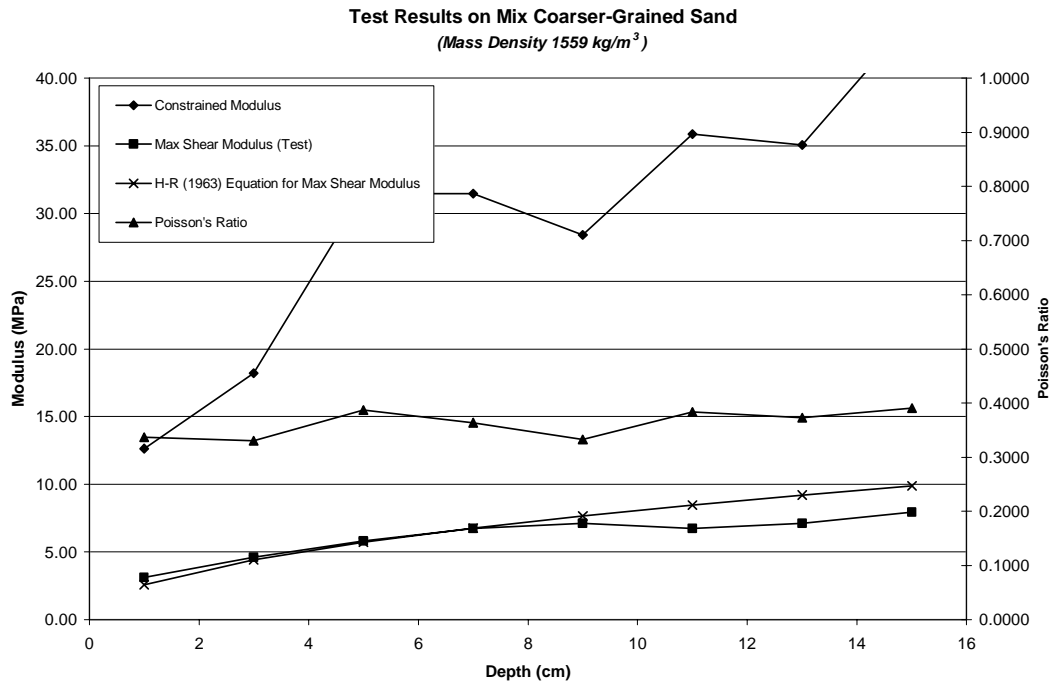**Figure 4.5**   Test results on dense coarse-grained sand.

The mass density for the loose soil samples was calculated to be approximately 1,400 kg/m^3 (87.4 lb/ft^3) while the dense samples had an apparent mass density of approximately 1,600 kg/m^3 (99.9 lb/ft^3). From the data recorded by the sensors on the cone penetrometer it can be seen that both the constrained modulus and the shear modulus generally increase with depth as the effective confining pressure increases. In addition, as the density of the samples increase, so too do the values for the constrained and shear modulus. Also shown in the graphs are the results from the calculations of a very well known empirical equation for the shear modulus of sands developed by Hardin and Richart in 1963. The shear modulus collected from the tests generally show very good agreement with the shear modulus from this equation. In addition, Poisson's ratio was calculated from the shear modulus and constrained modulus and is also included in the graphs. The graphs reveal that Poisson's ratio is generally between 0.3 and 0.4 which is very reasonable for the types of soils used (dry sands). Table 4.5, containing Poisson's ratio for different materials, is provided to compare with the resulting values for Poisson's ratio as determined from the test results.

Table 4.5   Poisson's ratio comparison.

Material	Range	Typical	Average Test Results
Loose sand or silty sand	0.2-0.4	0.3	0.36
Dense sand	0.3-0.45	0.35	0.35

As can be seen from the table the test results are in general agreement with typically accepted values for Poisson's ratio. For the dense sand samples, Poisson's ratio is 100% in agreement with the typical values of 0.35. For the loose samples, the Poisson's ratio is a little high, but still well within the given range.

4.4   Improvements Over Old System

As previously stated, the idea of the piezo-cone penetrometer was initially developed by Dr. Xiangwu Zeng of Case Western Reserve University. The original prototype for this device was developed in

2004 by a past graduate student of Case Western Reserve University, Lei Fu, under the advisement of Dr. Zeng. The original design is portrayed in the following picture.
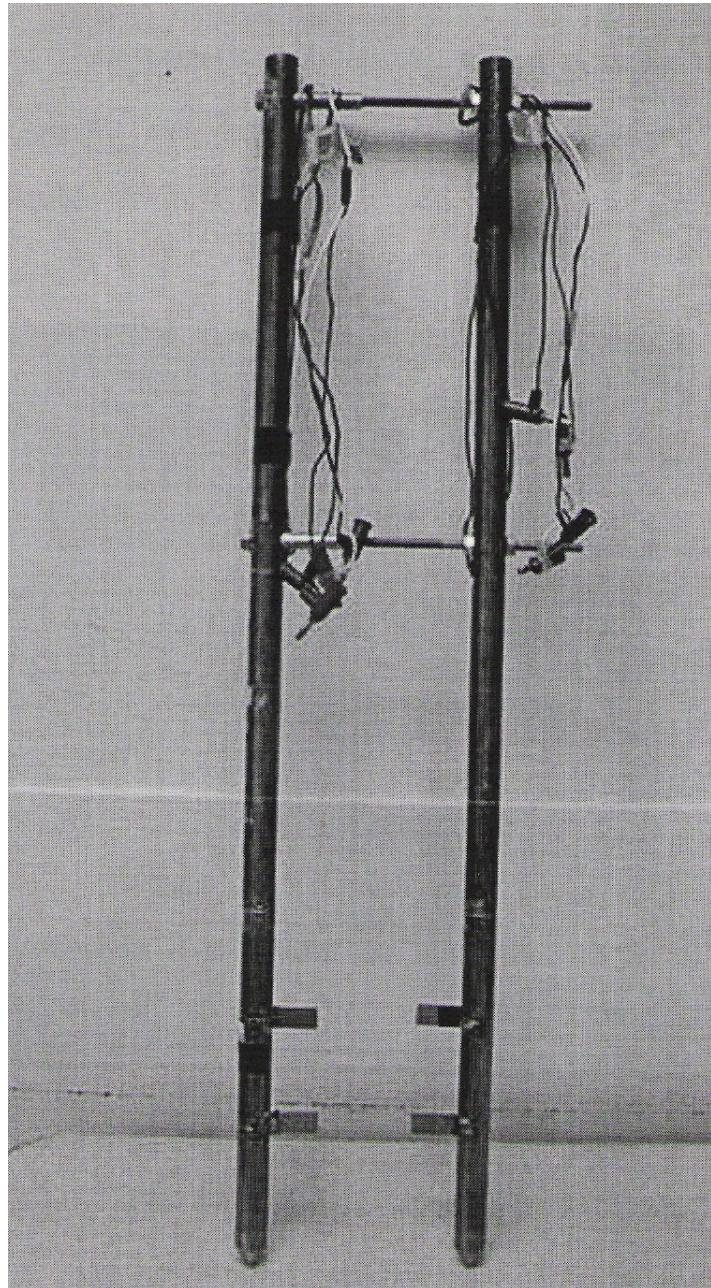

Figure 4.6   Original piezo-cone penetrometer developed by Fu in 2004.

This device was tested and also proved to produce reliable results for the shear modulus, constrained modulus, and Poisson's ratio of underlying soils of highway pavements. However, the system presented in this thesis has shown vast improvements over the original design.

First, the new prototype incorporates a solid shaft design versus the hollow tubes of the original design. This creates a much more solid design capable of withstanding the wear and tear of everyday use and multiple impacts created by the use of a vibratory hammer. Secondly, the sensors of the original design experience no protection from the penetrometers themselves. In the case that very stiff soils or gravel are encountered, the elements are liable to experience great damage as they are extremely fragile. The new system allows for the majority of the sensors to be enclosed within the penetrometers with only millimeters of the actual sensors jutting out. Also, the sensors are horizontally adjustable to provide optimization of the system while still providing protection to the sensors (see Figure 3.4). In addition, a horizontally adjustable leading edge is incorporated into the design directly below the bender element (see Figure 3.1). This edge does the work of pushing into the soils so that the exposed portion of the bender element remains protected. This edge is not provided below the extender element due to the fact that the extender element can be completely contained within the push rods. The operation of the extender element causes it to vibrate in a motion perpendicular to the push rods. This allows for them to be completely surrounded by the push rods, yet they are still able to "push" the soil and produce a strong and reliable p-wave. Third, this system can be completely waterproofed by inserting an o-ring between the two steel plates that make up the push rods. This allows for the system to work in all types of field and weather conditions. Fourth, the solid steel cone is removable. In case any damage or wear and tear occurs to the tip, it can be removed to be repaired or replaced. Finally, the push rods of the new system are calibrated and labeled in centimeters so that the depth of the elements under the soil can be easily and accurately read and recorded. Compared to the original piezo-cone penetrometer, this new system offers a much more solid, reliable, and field-ready design.

CHAPTER FIVE
SUMMARY, CONCLUSIONS AND IMPLEMENTATION PLAN

5.1   Overview and Conclusions

A newly improved piezo-cone penetrometer has been developed and constructed for the measurement of the soil stiffness of underlying soils of highway pavements. Bender and extender elements were implemented in the design to produce and receive s- and p-waves for the determination of the soil stiffness. Two different soils including Nevada sand and a coarser-grained sand were tested to determine the accuracy and reliability of this new device. The conclusions are as follows:

- The piezo-cone penetrometer has the potential to be used in the in-situ measurement of soil properties, such as the measurement of base and subgrade layer stiffness and Poisson's ratio during and after the construction of highway pavements.
- The piezo-cone offers accurate measurements of the shear modulus, constrained modulus, Poisson's ratio, and the elastic modulus of soils. These measurements can be taken simultaneously by this device and continuous profiles of these parameters can be obtained.
- The piezo-cone penetrometer test offers a new mechanistic approach for the quality control / quality assurance of pavement design and construction.
- Compared to empirical equations such as that of Hardin and Richart (1963) for the measurement of shear modulus, the piezo-cone penetrometer test is theoretically sound.
- The test is easy, quick, economical, reliable, and can be made mobile and automated for use in the field.

5.2   Suggestions for Further Study

There are many aspects left undiscovered in the study of the newly developed piezo-cone penetrometer. Suggestions for further study and improvement of the device include:

- Perform further testing on other various soil samples including other sands, gravelly soils, and clay, both dry and wet. This will ensure that the system will work in all types of field conditions and will validate the results.

- Develop a method to completely waterproof the system for all types of weather and field conditions.

- Develop an automated system that will allow one to easily switch from the bender to the extender elements when performing the tests.

- Continue to increase the strength of the signals for easy detection in the field and increase the protection of the sensors themselves as they are extremely fragile.

- Automated testing, data acquisition, and data processing system should be developed. The basic idea being that the system should consist of one mobile computer unit in addition to the piezo-cone penetrometer system itself. At the push of a button the system should be able to generate the pulse that triggers the transmitters and read the arrival time.

- Develop a user-friendly computer program to calculate the elastic modulus, shear modulus, constrained modulus, and Poisson's ratio based on the readings from the wave tests.

- Once the system is fault-proof, the idea of using this type of device on the moon or mars for soils testing should be implicated. In other words, research the idea of the development of a regolith penetrometer in hopes of determining the mechanical properties of the Lunar and Martian subsurface.

5.3   Implementation plan

When the new device is fully developed, we need to conduct pilot study at sites managed by ODOT. We need to conduct tests at one site of pavement under construction to check the quality of compaction and to determine mechanical properties of subbase and subgrade in situ. We also need to conduct tests on a section of existing pavement to measure the property of subbase and subgrade that have been in operation for a number of years. To use the device, two holes need to be cored through the pavement. If the field tests are successful, we can start using this device in selective projects in the state to build up experience and database. Then the results will be critically reviewed and the final implementation plan will be recommended.

The plan for implementation includes the following steps: 1) we will work with Pile Dynamics to further improve the design of the device and the data acquisition system for field use; 2) we will cooperate with ODOT to select two sites for field testing; 3) based on the results of field testing and feedbacks from

engineers, we will improve our design; and 4) we will conduct field demonstration of the device, develop users' manual, and train engineers for state-wide application of the device.

REFERENCES

[1] Abbiss, C.P. (1981). "Shear Wave Measurements of the Elasticity of the Ground." *Géotechnique*, London, 31(1), 91-104.

[2] APC International, Ltd. Piezoelectric Ceramics: Principles and Applications. Mackeyville, PA.: APC International, Ltd., 2002.

[3] Arulnahan, R., Boulanger, R.W., and Riemer, M.F. (1997). "Analysis of Bender Element Tests." *Geotechnical Testing Journal*, Vol. 21, No. 2, June 1998, pp. 97-105.

[4] Boulanger, R.W., Arulnahan, R., Harder, F.L., Jr., Torres, A.R., and Driller, W.M. (1998). "Dynamic Properties of Sherman Island Peat." *Journal of Geotechnical and Geoenvironmental Engineering*, ASCE, 124(1), 12-16.

[5] Bowles, Joseph E. Engineering Properties of Soils. Fourth Edition. Boston: Irwin McGraw-Hill, 1992.

[6] Burt, J.A., "The Electroacoustic Sensitivity of Radially Polarized Ceramic Cylinders as a Function of Frequency," *Journal of the Acoustical Society of America*. 64(6), 1640-1644 (1978).

[7] "California Bearing Ratio (CBR) and Road Pavement Design." The Idiot's Guide to Highway Maintenance. < http://www.highwaysmaintenance.com/cbrtext.htm > (13 May 2005).

[8] "Compaction." WAPA Asphalt Pavement Guide. < http://www.asphaltwa.com/wapa _web/modules/07_construction/07_compaction.htm > (9 May 2005).

[9] Croney, David, and Paul Croney. Design and Performance of Road Pavements. 3rd Edition. New York: McGraw-Hill, 1998.

[10] DeAlba, P., Baldwin, K., Janoo, V., Roe, G., and Celikkol, B., "Elastic-Wave Velocities and Liquefaction Potential," *Geotechnical Testing Journal*, GTJODJ, Vol. 7, No. 2, June 1984, pp. 77-87.

[11] "Dyamic Cone Penetrometer in Quality Control of Compaction, State-of-the-Art Report." Civil Engineering Database. < http://www.pubs.asce.org/www display. cgi?0489690 > (12 May 2005).

[12] Dyvik, R., and Madshus, C. (1985): "Lab Measurement of G_{max} Using Bender Elements," Advances in the Art of Testing Soils Under Cyclic Conditions, V. Koshla, ed, pp 186-196.

[13] "Falling Weight Deflection Testing." Dutch road Research Laboratories. < http ://www.koac-wmd.nl/gb-val.htm > (12 May 2005).

[14] "Falling Weight Deflectometer." Pavement Testing. < http://www.wsdot.wa.gov/ biz/mats/ pavement/fwd.htm > (12 May 2005).

[15] "History of Piezoelecticity." <u>Piezo Systems, Inc.</u> < http://www.piezo.com/history. html > (24 March 2005).

[16] Howarth, D.F., "Development and Evaluation of Ultrasonic Piezoelectric Transducers for the Determination of Dynamic Young's Modulus of Triaxially Loaded Rock Cores," *Geotechnical Testing Journal*, GTJODJ, Vol. 8, No. 2, June 1985, pp. 59-65.

[17] Huang, Yang H. <u>Pavement Analysis and Design</u>. 2nd Edition. New Jersey: Pearson Prentice Hall, 2004.

[18] "Introduction to Piezo Transducers." <u>Piezo Systems, Inc.</u> < http://www. piezo.com/bendedu.html > (29 December 2004).

[19] Jovicic, V., Coop, M.R., and Simic, M. (1996). "Objective Criteria for Determining G_{max} From Bender Element Tests." *Géotechnique*, London, 46(2), 357-362.

[20] Lawrence, F.V., Jr. (1963): "Propagation of Ultrasonic Waves Through Sand," Research Report R63-8, Massachusetts Institute of Technology, Cambridge, MA.

[21] Lawrence, F.V., Jr. "Ultrasonic Shear Wave Velocities in Sand and Clay," Research Report R65-05, Department of Civil Engineering, Massachusetts Institute of Technology, Cambridge, MA, 1965.

[22] "National Cooperative Highway Research Program – Completed Project." <u>NCHRP 1-37A</u>. < http://www4.nationalacademies.org/trb/crp.nsf/All+projects/NCHRP +1-37A > (10 May 2005).

[23] "NCHRP Project 1-37A: Development of the 2002 Guide for the Design of New and Rehabilitated Pavement Structures." <u>NCHRP 1-37A</u>. < http://www.ence.umd.edu/~schwartz/abstracts/nchrp_1_37a.html > (10 May 2005).

[24] NCHRP, Recommended Standard Method for Routine Resilient Modulus Testing of Unbound Granular/Base/Subbase Materials and Subgrade Soils, Protocol 1-28A (NCHRP, 2002).

[25] <u>Part II: Tests</u>. 16th Edition, "Standard Specifications for Transportation Materials and Methods of Sampling and Testing." Washington D.C.: American Association of State Highway Transportation Officials, 1993.

[26] <u>Resilient Modulus of Soils: Laboratory Conditions</u>. Edited by David J. Elton and Richard P. Ray. New York: American Society of Civil Engineers, 1989.

[27] Shirley, D.J. and L.D. Hampton (1978) "Shear Wave Measurements in Laboratory Sediments." *Journal of the Acoustical Society of America*, 63(2) February, pp. 607-613.

[28]   "Subgrade." <u>HAPI Asphalt Pavement Guide</u>. < http://www.hawaiiasphalt.com /HAPI/modules/06_design_factors/06_subgrade.htm > (11 May 2005).

[29]   Thomann, T.G. and Hryciw, R.D., "Laboratory Measurement of Small Strain Shear Modulus Under K_o Conditions," *Geotechnical Testing Journal*, GTJODJ, Vol. 13, No. 2, June 1990, pp. 97-105.

[30]   U.S. Department of Transportation, <u>Long-Term Pavement Performance Protocol P46: Resilient Modulus of Unbound Granular Base/Subbase Materials and Subgrade Soils</u> (McLean, Virginia: 1996), P46-1.

[31]   Viggiani, G., and Atkinson, J.H. (1995). "Interpretation of Bender Element Tests." *Géotechnique*, London, 45(1), 149-154.

[32]   Zeng, X., Figueroa, J.L. and L. Fu. (2003b) "Measurement of Base and Subgrade Layer Stiffness During and After Construction Using a Cone Penetrometer Equipped with Piezoelectric Sensors." <u>Proceedings of the International Conference on Highway Pavement Data, Analysis and Mechanistic Design Applications</u>. Volume 2. September, Columbus, Ohio.

[33]   Zeng, X., Figueroa, J.L. and L. Fu. (2004) "Measurement of Base and Subgrade Layer Stiffness Using Bender Element Technique." <u>Recent Advances in Materials Characterization and Modeling of Pavement Systems</u>. Special Publication 123, pp. 35-45.

[34]   Zeng, X. and B. Ni (1998). Application of Bender Elements in Measuring G_{max} of Sand Under K_o Condition. *Geotechnical Testing Journal*, ASTM, Vol. 21, No. 3, pp. 251-263.

[35]   Zeng, X. and B. Ni (1999). Stress-Induced Anisotropic G_{max} of Sands and Its Measurements, ASCE *Journal of Geotechnical and Geoenvironmental Engineering*, Vol. 125, No. 9, pp. 741-749.